



1 mLDNDCv1.0: A Machine Learning-based Surrogate of 2 LandscapeDNDC for Optimising Cropping Systems in Denmark

3
4 Meshach Ojo Aderele^{1,2}, Edwin Haas³, Licheng Liu⁴, João Serra^{1,2,5}, David Kraus³, Klaus Butterbach-
5 Bahl^{1,2,3}, Jaber Rahimi^{1,2,3*}

6
7 ¹ Pioneer Center Land-CRAFT, Department of Agroecology, Aarhus University, Aarhus, Denmark

8 ² Department of Agroecology, Aarhus University, Blichers Allé 20, 8830 Tjele, Denmark

9 ³ Institute of Meteorology and Climate Research, Atmospheric Environmental Research (IMK-IFU),
10 Karlsruhe Institute of Technology (KIT), Garmisch-Partenkirchen, Germany

11 ⁴ Department of Bioproducts and Biosystems Engineering, University of Minnesota, St. Paul, MN 55108,
12 USA.

13 ⁵ Forest Research Centre CEF, Associate Laboratory TERRA, Instituto Superior de Agronomia,
14 Universidade de Lisboa, 1349-017, Lisbon, Portugal

15
16 * Correspondence to: Jaber.rahimi@ago.au.dk

17 18 Abstract

19 Optimising Danish arable management is critical for reducing greenhouse-gas (GHG) emissions and
20 nitrogen (N) losses while maintaining or even improving crop productivity and soil health. Process-
21 based models such as LandscapeDNDC can simulate the effects of management on agroecosystem
22 functioning. However, their computational demand limits large-scale optimisation. Here we present
23 mLDNDCv1.0, a tree-based machine-learning surrogate of LandscapeDNDC that allows for the rapid
24 exploration of large decision spaces without sacrificing mechanistic fidelity. We generated a synthetic
25 training set of >45 million LandscapeDNDC simulations from a full factorial of soils, climate (2011-2020),
26 and management options for winter wheat. We benchmarked gradient-boosted tree algorithms
27 (LightGBM, XGBoost, CatBoost) on predictive performance. XGBoost delivered the most accurate and
28 stable predictions for the core indicators in this study: soil N₂O emissions (R² = 0.81), NO₃⁻ leaching (R²
29 = 0.84), yield (R² = 0.93), and for soil-organic-carbon stock changes (R² = 0.86). The model maintained
30 high accuracy when confronted with real management and environmental settings that reflected true
31 operating conditions. Coupling mLDNDC with the multi-objective evolutionary algorithm NSGA-II
32 allowed us to optimise millions of management combinations across all winter wheat fields in Denmark.
33 Pareto-optimal solutions reduced N₂O emissions by 27.5 ± 4.5 %, NO₃⁻ and leaching by 27 ± 3.0 %.
34 These solutions also increased grain yield by 8.5 ± 1.5 % and soil-organic-carbon stocks by 1.2 ± 0.1 %,
35 and improving nitrogen-use efficiency (NUE) by 10 ± 2 %, while turning the system into a net GHG sink
36 (2200 ± 400 Mg CO₂-eq ha⁻¹ yr⁻¹). These gains were achieved without increasing total fertiliser input.
37 They arose from re-allocating mineral and organic fertiliser N input, adjusting incorporation depth, and
38 optimising residue, catch-crop, and irrigation practices. Thus, mLDNDC therefore provides a scalable,
39 transparent framework for country-wide optimisation and real-time decision support in climate-smart
40 agriculture.

41 42 1. Introduction

43 Optimising cropping systems is critical for increasing agricultural productivity while reducing
44 environmental impacts. Agriculture accounts for 20–25 percent of global anthropogenic greenhouse
45 gas (GHG) emissions and is a major driver of climate change (Vermeulen et al., 2012). In Denmark,
46 where agriculture covers more than 55% of the total land area (Hansen et al., 2025), improving
47 management practices is both necessary and urgent. The Danish agricultural sector plays a central role
48 in national food, yet it is also responsible for about 23% of national greenhouse gas emissions (Nielsen
49 et al., 2020), while being a major contributor to nutrient runoff and land-use pressures (Pugliese et al.,



2023). As global demand for food continues to rise, Danish agriculture faces the dual challenge of sustaining high yields while meeting environmental and climate commitments. Without optimisation, farming systems risk becoming inefficient and environmentally unsustainable (Wezel et al., 2020). Variability in soil conditions, weather patterns, and management intensity often leads to uneven resource use and suboptimal productivity (Abdu et al., 2023). Moreover, climate change is intensifying these challenges by altering growing conditions and increasing the frequency of extreme events such as droughts and floods (Baker & Anttila-Hughes, 2020). This makes it increasingly important to identify management strategies that can maintain productivity, enhance resilience, and reduce environmental footprints. For exploratory scenario testing, process-based models (PBMs) such as LandscapeDNDC (LDNDC) (Haas et al., 2013) — remain the tools of choice. PBMs represent the biophysical and biogeochemical processes that regulate crop growth, soil dynamics, water balance, and nutrient cycling (Zhang et al., 2022). By explicitly simulating interactions among crops, soils, and the atmosphere, they improve system understanding, challenge theoretical assumptions, and predict responses to management or climate drivers (Jeong et al., 2020). When run across diverse environments, PBMs quantify trade-offs among yield, nitrogen losses, GHG emissions, and soil-carbon dynamics, thereby providing a science-based foundation for sustainability assessments (Shi et al., 2025). Yet the same mechanistic richness that gives PBMs their credibility also makes them computationally heavy, especially when thousands of management permutations must be tested at national scale (Lu et al., 2019). Machine-learning (ML) methods can overcome the runtime barrier, but, when used in isolation, they lack an intrinsic grasp of soil–plant–atmosphere processes. Merging ML with PBMs therefore offers an attractive compromise of process realism with substantial speed-ups (Droutsas et al., 2022). One promising avenue is surrogate (or meta-) modelling, in which an ML algorithm is trained on PBM outputs, and subsequently emulates the PBM at a fraction of the computational cost (Aderale et al., 2025). Surrogate techniques are now being increasingly adopted across agri-environmental sciences (e.g., Aderale et al., 2025). Applications include predicting crop yield (Nguyen et al., 2019; Shahhosseini et al., 2019), gaseous-nitrogen fluxes such as nitrous oxide (N₂O) and ammonia (NH₃) (Perlman et al., 2014; Villa-Vialaneix et al., 2012), assessing nitrate-leaching (Piñeros Garcet et al., 2006), studying the terrestrial carbon-cycle (Luo et al., 2011; Xiao et al., 2022), investigating crop physiology and water dynamics (Attia et al., 2022), or grasslands (Pylianidis et al., 2022). However, these efforts have largely focused on field or landscape-scale applications and often target single sustainability indicators. To date, no study has carried out a nationwide optimisation of agriculture that simultaneously considers yield, nitrous oxide (N₂O) emissions, nitrate (NO₃⁻) leaching, and soil organic carbon (SOC) dynamics. Building on this gap, the present work addresses two questions: (i) can a functional machine learning-based surrogate model be developed for LandscapeDNDC, and (ii) can such surrogates be used to optimise Danish agriculture at national scale in a way that reduces environmental impacts while enhancing productivity and soil health, without compromising scientific rigour? Danish agriculture is used as a case study due to data availability, while the methodology is general and can be applied to other countries, continents, or even global-scale analyses. Filling these gaps demands both an accurate biogeochemical representation and an optimisation engine capable of searching a vast management decision space. Exploratory scenario applications, where a range of management options are defined and simulated using PBMs, remain an interesting and potentially useful option (Aderale et al., 2025). While informative, such “fixed-scenario” approaches restrict discovery to strategies already envisioned. Search-based optimisation, by contrast, defines broad decision boundaries and allows an algorithm to find novel solutions within them. This paradigm has been applied to climate-smart crop production elsewhere (Xiao et al., 2024) and is adopted here. Coupling an evolutionary optimiser with a PBM such as LandscapeDNDC would require thousands to millions of simulations, rendering the process impractical. Therefore we introduce mLDNDC, a machine-learning surrogate of LandscapeDNDC that preserves mechanistic fidelity while reducing computation

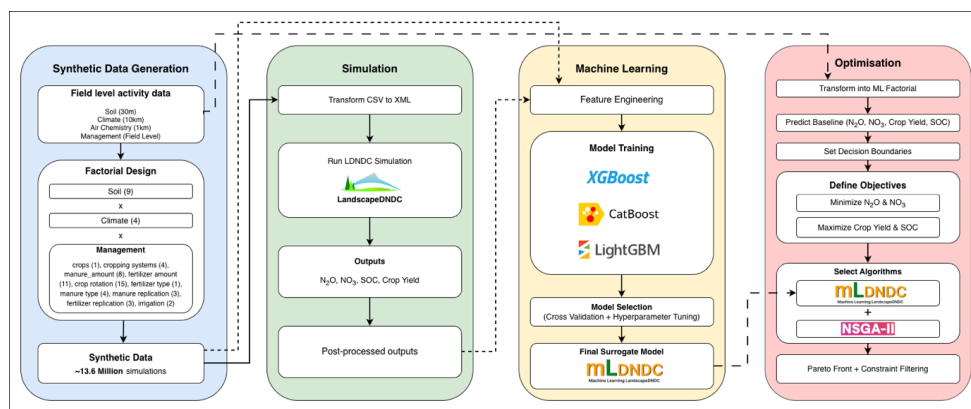


101 time. mLDNDC allows for the thorough exploration of management options and, when paired with an
102 optimiser, can identify strategies that improve productivity, resilience and environmental sustainability.
103 This study showcases mLDNDC application to winter wheat, the most widely grown and economically
104 important cereal in Denmark (Barua et al., 2014), accounting for over 23% of the cropping area, and
105 demonstrate its use in optimising management under contemporary Danish conditions. The analysis
106 tracks four core outputs: N₂O emissions, NO₃⁻ leaching, grain yield, and SOC change. Together, these
107 variables capture the essential balance between productivity and environmental impact, forming the
108 basis of our optimisation exercise.

109 2. Methods

110 This study was conducted through four main stages, summarized in Figure 1. The workflow comprised
111 (i) Synthetic data generation for winter wheat at field level in Denmark, (ii) Simulation using
112 LandscapedDNDC, (iii) Training of machine learning models on the synthetic input–output datasets
113 produced by LandscapedDNDC, and (iv) Optimization, where the trained surrogate model was applied
114 to achieve the study objectives.

115
116
117
118



119
120
121

Figure 1. Overview of the methodological framework for developing mLDNDC and its application for optimising cropping systems in Denmark.

122 2.1. Synthetic Data Generation

123 Developing a robust surrogate model demands a dataset that goes beyond what is available from field
124 observations. Although empirical data is valuable, it only covers a narrow slice of the management
125 practices currently used, missing much of the plausible decision space needed for trade-off analysis and
126 optimisation. We bridge this gap by creating a synthetic dataset that combines observed and
127 hypothetical management scenarios. This broader coverage enables the surrogate model to generalise
128 beyond management boundaries of current management practices.

129 The construction of the dataset involved two steps. First, we defined plausible ranges for numeric
130 predictors (e.g., fertiliser amount) and alternative possibilities for categorical (e.g., fertiliser type)
131 options for all key management variables, drawing on field-level records and agronomic knowledge.
132 Second, we varied these variables within their agronomic limits using a full factorial design to generate
133 a large set of unique management combinations that represent both current practice and potential
134 future strategies.

135 2.1.1. Field Level Activity Data

136 We used the harmonized field-level data from the SmartField project to drive the process-based model
137 representing Danish agriculture. This dataset was developed to generate the Tier-3 GHG emission
138 inventory (Rahimi et al., in preparation) and the dataset was used as baseline to represent variations in
139



140 crop sequences and rotations and management practices (e.g., fertilisation, irrigation, tillage, cover
141 cropping, and residue management).

142 The dataset is based on information on crop types and cropland boundaries available at field scale from
143 2011 to 2020 from the General Farm Register (Rolighed, 2023), combined with total amounts of
144 synthetic (e.g., ammonium-based inputs) and organic (e.g., livestock slurry) fertilizers reported at the
145 farm scale. The fertiliser inputs were distributed to fields within each farm based on the allowed rates
146 for specific crop and soil types defined by the Danish AgriFish Agency to fulfill national regulations
147 (Dalgaard et al., 2014).

148 Management boundaries were identified to represent the observed range of current agricultural
149 practices in Denmark. These boundaries served as reference points for defining the limits of each
150 management variable. A management library was then constructed, encapsulating all possible
151 combinations of these management parameters for further use in the factorial design stage.

152 2.1.2. Factorial Design

153 The factorial design was developed to generate a comprehensive and representative set of synthetic
154 management scenarios. This was accomplished by systematically combining soil, climate, crop
155 management, and fertilisation.

156 **Soil (9 levels):** Soil properties, including texture, soil organic carbon (SOC) and bulk density (BD), were
157 extracted as geospatial raster layers at 30.4 m resolution for five standard depth intervals (0–5, 5–15,
158 15–30, 30–60 and 60–100 cm). Soil pH for the same depths was obtained from a separate dataset at
159 100 m resolution. Saturated hydraulic conductivity (K_s) was derived using a pedotransfer function based
160 on relevant soil attributes (Rahimi et al., 2024). The soil classes used for factorial design was derived
161 from a 30 m resolution national soil map classified according to the Jordbær soil classification system
162 in Denmark (Figure S.2). This classification system resulted in 9 distinct soil classes that represent the
163 dominant soil types in Danish agricultural landscapes.

164 **Climate (4 levels):** Climate data, including (daily mean air temperature, global radiation, and
165 precipitation) were obtained from the Danish Meteorological Institute (DMI) at a spatial resolution of
166 10 km (<https://www.dmi.dk/>). The DMI IDs were categorized into 4 climate zones based on the De
167 Martonne aridity index (Figure S.3), capturing the spatial variability of moisture availability and its
168 potential impact on crop growth and soil processes (e.g., potential evapotranspiration). To simulate the
169 synthetic dataset, one DMI ID was randomly selected from each class. For atmospheric N deposition,
170 regional-scale outputs from the atmospheric chemical transport model, the Danish Eulerian
171 Hemispheric Model (Rahimi et al., 2024), were used to provide nitrogen deposition inputs for our
172 model. For simulation purposes, the air-chemistry inputs were taken from the same randomly selected
173 DMI ID.

174 **Cropping Systems (4 levels):** Cropping systems were adapted from Aderle et al. (2025) and represent
175 different combinations of crop residue and catch crop management. Four distinct categories were
176 defined: (i) complete residue removal without a catch crop, (ii) complete residue retention with a catch
177 crop, (iii) complete residue removal with a catch crop, and (iv) complete residue retention without a
178 catch crop. For all cropping systems, tillage was carried out five days before crop establishment to
179 prepare the seedbed. These combinations capture the most relevant residue–catch crop interactions
180 observed in Danish agricultural systems.

181 **Fertilization amount (11×8 levels):** Synthetic fertilizer application rates were defined in 30 kg N ha⁻¹
182 increments from 0 to 330 kg N ha⁻¹, resulting in 11 levels. Organic fertilizer application rates followed a
183 similar structure, ranging from 0 to 240 kg N ha⁻¹ in 30 kg intervals, resulting in 8 levels. The upper
184 bounds for both fertilizer types were intentionally set higher than the maximum levels typically
185 observed in national practice to allow simulations beyond the baseline and support optimisation and
186 sensitivity analyses.

187 **Fertilization type (1×4 levels):** Ammonium nitrate (NH₄NO₃-) was selected as the sole synthetic fertilizer
188 type as it accounts for dominant share of the total synthetic fertilisers used in Denmark. Four organic
189 fertilizer types were considered: compost, farmyard manure, slurry (injected), and slurry (surface
190 applied).



191 **Fertilization splits (3x3 levels):** Both synthetic and organic fertilization were represented by three
192 application-frequency levels (one to three applications per growing season). For each synthetic
193 scenario, the corresponding organic scenario was combined to create realistic split combinations. To
194 ensure realistic application timing, data from the Danish catchments from the National Monitoring
195 Program for Water Environment and Nature, NOVANA (LOOP-program; In Danish:
196 Landovervågningsprogrammet) was used for the timing and per-split rates. One matching field-year
197 was randomly selected from this dataset for each synthetic management record. For example, if a
198 winter wheat scenario in 2017 required one organic split and two synthetic splits, a field-year with the
199 same split structure (1 organic + 2 synthetic) would be randomly selected from the dataset and its
200 observed timing and per-application rate pattern would be adopted. This approach preserves realistic
201 within-season fertilization schedules while allowing for the systematic exploration of total N levels.

202 **Crop Rotation (15 levels):** Crop rotations were defined using a two-year rotation system that precede
203 the main crop, winter wheat. Five primary crop categories were considered: cereals, legumes, leafy
204 crops, root crops, and grasses. Combining these categories across two preceding years produced 15
205 unique rotation types, ensuring a broad range of agronomic sequences was represented (Figure S.4).

206 **Irrigation (2 levels):** We represented irrigation as a binary factor (irrigated vs. non-irrigated), and
207 triggered applications based on crop water demand. This was preferred to dynamically calculating
208 irrigation needs according to climate x management interactions to reduce the number of factorial
209 scenarios and its computational demand both for LDNDC and ML.

210 Although a factorial design is comprehensive by nature, it can generate unrealistic or inconsistent
211 combinations. For example, very high fertilization levels may not be agronomically plausible when
212 represented with a single split as e.g. certain synthetic–organic pairings can produce excessively high
213 total N inputs. When amount of organic fertilizer is zero, the “type” of an organic fertilizer is not
214 meaningful. Therefore, the synthetic dataset was systematically screened and cleaned using rule-based
215 plausibility checks to eliminate such combinations and ensure that the remaining scenarios reflect
216 realistic and interpretable management configurations.

217 **2.2. Simulation With LandscapeDNDC**

218 The synthetic data generation process produced approximately 13.6 million rows, which were
219 subsequently reduced to about 4.5 million rows per simulation year during preprocessing (Table S.3).
220 This yielded a total of about 45 million rows spanning the ten-year period from 2011 to 2020. These
221 rows served as the input dataset for the simulation stage. All simulations were performed using the
222 LandscapeDNDC.

223 **2.2.1. Process-based Model Description**

224 LandscapeDNDC (LDNDC) is a process-based framework that simulates the coupled cycles of carbon,
225 nitrogen, and water cycles in cropland, grassland, and forest systems (Haas et al., 2013). It links five
226 core modules: (i) PlaMo^x for crop growth (Kraus et al., 2016; Liebermann et al., 2019); (ii) CanopyECM
227 for micro-climate processes (Grote et al., 2009); (iii) WatercycleDNDC for soil water and hydrology
228 (Kiese et al., 2011); (iv) AirchemistryDNDC for atmospheric chemistry; and (v) MeTr^x for soil
229 biogeochemistry (Kraus et al., 2015).

230 The model has been applied and tested in a range of contexts. Across Europe, Haas et al. (2022)
231 explored long-term residue-management effects on soil organic carbon (SOC) and N₂O emissions. Kraus
232 et al. (2022) validated national-scale simulations in the Philippines for alternate wetting and drying in
233 rice systems, while Smerald et al. (2023) used LDNDC to examine global nitrogen-redistribution options
234 for closing yield gaps with minimal environmental damage.

235 For its application in Danish conditions, LDNDC has undergone detailed calibration and testing. Kollmer
236 (2023) calibrated plant-physiological and soil parameters using data from the long-term Askov
237 experiment and successfully reproduced the observed SOC accumulation in dependence of different
238 field management regimes. Grados et al. (2024) compared modelled N₂O fluxes with field
239 measurements from the Foulum and reported a standardised RMSE of 2.03 g N₂O-N ha⁻¹ d⁻¹. Rahimi et al.
240 (2024) evaluated LDNDC across the six LOOP catchments in Denmark and achieved an overall R² of
241 0.77 for yield predictions. The present study adopts the same parameter bounds and input settings as



242 used in the listed studies. Finally, Aderere et al. (2025) assessed twelve alternative Danish cropping
243 regimes combining fertiliser, residue, and catch-crop strategies. They analysed trade-offs among GHG
244 emissions, nitrogen leaching, SOC changes, and yield.
245 Given the extensive international and Danish level validation, LDNDC provides a robust, well-tested
246 foundation for the surrogate-modelling work carried out here.

247 **2.2.1. Process-based Model Simulation**

248 The simulations covered the period from 2011–2020 and focused on winter wheat. Next, we converted
249 the generated synthetic management scenarios (Section 2.1.2) to LDNDC data requirements in
250 Extensive Markup Language (XML). We took planting dates, harvest dates, and fertiliser schedules from
251 the field-level activity dataset described in [Section 2.1.1](#), so that model settings would reflect typical
252 Danish practices across the main cropping regions. Every synthetic management combination from the
253 factorial design was run as a separate LDNDC job. To manage the large workload, we used an HPC
254 cluster, launching 40 parallel tasks, each with one (CPU cores each, 600 GB shared memory). With this
255 setup the full batch finished in roughly seven days; running on a desktop machine would have taken
256 several weeks.

257 LDNDC was configured for daily time steps, but the simulations were run at subdaily intervals,
258 generating outputs for N₂O emissions, NO₃⁻ leaching, grain yield, and changes in soil organic carbon
259 (SOC).

260 **2.3. Machine Learning**

261 **2.3.1. Feature Engineering**

262 Developing the surrogate model required a comprehensive set of predictor variables capturing the key
263 biophysical, climatic, and management processes that regulate crop performance, nitrogen dynamics,
264 and soil-carbon outcomes. These features were derived from LDNDC simulations and combined with
265 processed soil and climate data. They were engineered to represent both long-term system
266 characteristics and short-term, management-sensitive drivers.

267 **Management practices:** One primary management variable, additional feature such as total nitrogen
268 input, was calculated by summing all mineral fertiliser nitrogen and manure nitrogen applied within a
269 given year; this measure represents the total nitrogen supply entering the cropping system and is a
270 critical determinant of crop productivity, nitrate leaching, and nitrous oxide emissions. To capture
271 nonlinear response behaviour associated with nitrogen inputs, a squared term or second order
272 polynomial of total nitrogen and each manure and synthetic fertiliser inputs were also included as an
273 additional feature ([Sutton & Matheus, 1991](#)).

274 **Climate:** To characterise rainfall patterns, we constructed a rainfall-frequency indicator by counting the
275 number of days per year with measurable precipitation. This captures moisture intermittency which
276 strongly influences soil mineralisation, denitrification, and crop-growth cycles. A suite of additional
277 climate variables were engineered to capture both seasonal and crop-stage specific conditions,
278 including annual precipitation, total precipitation during the crop's growing season, and seasonal
279 precipitation for autumn, winter, and spring; equivalent temperature metrics—mean annual
280 temperature and mean temperatures for the growing season and each major season—were generated
281 to reflect the climatic environment governing crop development, soil biological activity, and nitrogen
282 turnover.

283 **Short-term climate effects:** Short-term hydrological conditions surrounding nutrient applications were
284 incorporated through event-based precipitation indicators that quantify accumulated rainfall in the
285 seven days preceding each fertiliser and manure application. We also included rainfall in the three days
286 following each application to capture conditions that influence nitrogen-loss pathways such as
287 volatilisation, rapid infiltration, or surface runoff. These pathways are known to affect both nitrate
288 leaching and nitrous oxide emissions.

289 **Soil:** We constructed soil features by aggregating the properties of the upper three soil layers (0-20cm
290 depth), which represent the active root zone most relevant for crop growth and nutrient cycling. We
291 calculated the mean values of field capacity, wilting point, sand, silt, and clay fractions, organic carbon,
292 organic nitrogen, pH, bulk density, and saturated hydraulic conductivity for each field. These aggregated



293 variables provide a representative profile of the soil's physical and biogeochemical characteristics to be
294 used in the surrogate model.

295 **Target variables:** The target variables were transformed prior to training recognising that variable
296 transformation is a well-established strategy for improving the performance of supervised-learning
297 models when target variables are highly skewed or exhibit heteroscedasticity. Nitrous oxide emissions,
298 nitrate leaching, and crop yield were log-transformed to address strong skewness. Soil-organic-carbon
299 change was transformed using the Yeo–Johnson power-transformation method (Weisberg, 2001) to
300 accommodate both positive and negative values, .

301 The full list of features used for the model training can be found in [Table S.4](#).

302 **2.3.1. Model training**

303 **2.3.1.1. Benchmarking**

304 The dataset was split into two parts: 80 % used for model training, and the remaining 20 % was withheld
305 for an independent test of generalisation performance. This ratio is widely adopted in machine-learning
306 practice because it balances the data available for learning with the need for reliable evaluation (Kuhn
307 & Johnson, 2013).

308 To identify the most suitable surrogate model for the target variables agro-ecosystem indicators, three
309 gradient-boosting decision-tree algorithms ([Section S.1](#)) were benchmarked: LightGBM, XGBoost, and
310 CatBoost. Light Gradient Boosting Machine (LightGBM; Ke et al., 2017) accelerates training via
311 histogram-based splits and leaf-wise growth; Extreme Gradient Boosting (XGBoost; Chen & Guestrin,
312 2016) adds regularisation, parallel execution, and efficient sparse-matrix handling; and CatBoost
313 (Prokhorenkova et al., 2017) employs ordered boosting with target statistics to mitigate overfitting and
314 handle categorical inputs. First, each candidate model was initially trained using its default
315 hyperparameters ([Table S.1](#)), and baseline performance was evaluated on the test set. Based on this
316 initial comparison, the best-performing algorithm was selected and subsequently subjected to intensive
317 hyperparameter tuning combined with further cross-validation. This staged workflow avoids
318 unnecessary optimisation of weaker candidates and substantially reduces computational cost while
319 maintaining methodological rigour in model selection and evaluation.

320 **2.3.1.2. Hyperparameter Tuning**

321 Hyper-parameter optimisation was carried out with Optuna (Akiba et al., 2019), which uses a Tree-
322 structured Parzen Estimator (TPE) Bayesian-optimisation engine coupled with early-stopping “pruners”
323 to traverse the search space efficiently. The objective function minimised the validation error, and wall-
324 clock time was kept in check by running each trial on a random 1 % subsample of the training data to
325 reduce the tuning time and computational requirements. This choice follows the findings of Kapoor and
326 Amazon (2021), who showed that tuning on as little as 1 % of a large dataset yields validation-metric
327 differences below 0.5% relative to tuning on the full dataset.

328 Once the hyperparameter search converged, the selected configuration was used to train the selected
329 model using five-fold cross-validation on the full dataset. The data were randomly shuffled and
330 partitioned into five equally sized folds; in each iteration, four folds were used for training and the
331 remaining fold served as validation. This procedure ensured that every observation contributed to both
332 model fitting and validation, providing robust estimates of predictive performance. Reported
333 performance metrics were derived from the cross-validation results.

334 After confirming stable performance across folds, the final surrogate model was trained on the
335 complete dataset using the optimised hyperparameters. This final refit maximised the use of available
336 information and produced the mLDNDC model used for downstream large-scale prediction and
337 management optimisation. This is consistent with standard practice when the objective is the
338 operational deployment of a single, fully trained model (Hastie et al., 2009).

339 **2.3.1.3. Model Explanation**

340 To interpret the relative influence of management and environmental variables on each agro-
341 ecosystem indicator, we computed SHapley Additive exPlanations (SHAP) values for the optimised
342 XGBoost models. Using TreeSHAP (Lundberg & Lee, 2017), each prediction was decomposed into
343 additive feature attributions whose magnitudes indicate the strength of the effect and whose signs



344 indicate the direction (positive or negative) of the contribution, thereby offering a consistent, locally
345 accurate measure of variable importance across the entire dataset.

346 **2.3.1.4. Model Validation**

347 To ensure the generalizability and external validity of the surrogate model, an independent validation
348 was performed using data not involved in model training or simulation by LandscapeDNDC. For this
349 purpose, national-scale crop yield data obtained from the National Statistics Denmark were employed
350 as an external benchmark. This dataset represents real-world observations across diverse management
351 and environmental conditions, providing a robust basis for evaluating model transferability beyond the
352 simulation domain.

353 **2.4. Optimisation**

354 **2.4.1. Decision Boundaries**

355 The optimization process was constrained within predefined decision boundaries, representing the
356 range of controllable management variables. These boundaries define the feasible search space for
357 identifying optimal agroecosystem management strategies.

358 Specifically, the manure application rate was varied from 0 to 210 kg N ha⁻¹, and the synthetic fertilizer
359 rate ranged from 0 to 300 kg N ha⁻¹. These ranges were selected to encompass the typical and extreme
360 management practices observed in Danish cropping systems while ensuring agronomic plausibility.

361 Categorical management factors, as described in [Section 2.1.2](#), were also included in the optimization
362 search space. These comprised crop rotation, cropping systems, synthetic fertilizer types, manure
363 types, replication schemes (for both manure and synthetic fertilizer, showing how many times they
364 were applied), irrigation, and manure depth. Optimizing these continuous and categorical decision
365 variables allows the optimization framework to capture a broad spectrum of feasible management
366 combinations aimed that balance productivity and environmental outcomes.

367 The optimisation was conducted at the individual winter wheat field level across Denmark using
368 national inventory data, with results subsequently aggregated to a 10 km × 10 km grid to facilitate
369 spatial visualisation. Accordingly, the baseline represents the current, field-specific management
370 practices and associated outcomes under current farming conditions.

371 **2.4.2. Objectives**

372 The optimization problem was formulated as a multi-objective task aimed at simultaneously improving
373 environmental and agronomic outcomes. Specifically, the objectives were to minimize N₂O emissions
374 and NO₃⁻ leaching, while maximizing crop yield and SOC change.

375 These four objectives collectively represent the key dimensions of sustainable agricultural
376 management, enhancing productivity while mitigating greenhouse gas emissions and nutrient losses
377 The formulation can be expressed as:

378 Minimize (f_1, f_2) = (N₂O emissions, NO₃⁻ leaching)

379 Maximize (f_3, f_4) = (Crop yield, SOC change)

380 There is no explicit weighting scheme applied to the target variables; in the current setup, none of the objectives
381 is prioritized over the others, so N₂O, NO₃⁻, yield, and annual SOC are all treated equally.

382 The multi-objective optimization was conducted under the decision boundaries defined in [Section](#)
383 [2.4.1](#), allowing the identification of Pareto-optimal solutions that represent trade-offs between
384 environmental protection and agricultural productivity.

385 **2.4.3. Optimisation Algorithm**

386 The Non-dominated Sorting Genetic Algorithm II (NSGA-II) (Deb et al., 2002) was employed to solve the
387 multi-objective optimization problem. NSGA-II is a widely adopted evolutionary algorithm designed for
388 identifying Pareto-optimal solutions in problems with conflicting objectives. It maintains population
389 diversity through a crowding distance mechanism and ensures computational efficiency via fast non-
390 dominated sorting.

391 The implementation was carried out in Python using the pymoo optimization framework (Blank & Deb,
392 2020). Each generation of the algorithm evolved candidate management strategies through processes
393 of selection, crossover, and mutation, iteratively improving the trade-offs between environmental and
394 productivity objectives. The algorithm efficiently explored the multi-dimensional decision space defined
395 in [Section 2.4.1](#), identifying optimal combinations of manure rate, fertilizer rate, and other categorical



396 management variables that balanced N₂O emissions, NO₃⁻ leaching, crop yield, and SOC change. At the
397 end of the optimization, the pareto front is returned which is the top 50 management practices that
398 fulfils our objectives for a specific field.

399 **2.4.4. Constraint Based Filtering**

400 After generating the Pareto-optimal solutions for each field, a constraint-based filtering step was
401 applied to identify management strategies that are both environmentally beneficial and agronomically
402 feasible. Two sets of constraints were used in this study.

403 The first ensured that any selected management strategy outperformed the field's current baseline.
404 Specifically, an optimised solution was retained only if it produced lower nitrous oxide emissions and
405 lower nitrate leaching, while achieving a higher crop yield and greater soil organic carbon content than
406 the baseline management for that field. This requirement ensured that the recommended solutions
407 would deliver clear improvements in all key sustainability indicators rather than merely shifting
408 environmental.

409 The second constraint addressed regional manure-use feasibility. To reflect realistic resource
410 availability, the total manure applied in any optimised solution was required to remain at or below the
411 total manure availability for the corresponding NUTS2 region in Denmark. This ensured that the
412 optimisation results did not rely on manure inputs that exceed what is currently accessible within
413 regional nutrient cycling systems.

414 These constraints guaranteed that the final set of optimised management strategies were both
415 environmentally superior and grounded in practical resource limitations, thereby increasing the
416 likelihood of real-world applicability and policy relevance.

417 **2.5. Performance evaluation**

418 Model performance was evaluated using the coefficient of determination (R²) and the root mean
419 square error (RMSE) to quantify both predictive accuracy and the magnitude of prediction error. It
420 should be noted that this assessment was conducted in two phases, each of which aligned with the
421 conceptual distinction between the possibility space and the actual space of management practices.

422 The first phase (possibility space) measured training accuracy by evaluating the model on the same
423 synthetic dataset used for model development. This dataset represents the "possibility space", which
424 encompasses the full range of management combinations that could theoretically occur. The aim was
425 to determine how well the model captures relationships within this synthetic generated domain.

426 The second phase (actual space) measured validation accuracy using an independent dataset derived
427 from reported national field management records for winter wheat. This dataset reflects the "actual
428 space" i.e., the management practices that have been implemented under real-world conditions, and
429 all the necessary response variables for this dataset were produced through LDNDC simulations.
430 Consequently, this phase provides a more realistic test of the model's generalizability, since it evaluates
431 performance under the management strategies that occur in practice rather than only in theory.

432 **2.6. GHG Balance Calculation**

433 The soil net greenhouse gas (GHG) balance was estimated to evaluate the overall climate impact of the
434 baseline and optimised cropping system. The balance was calculated as the difference between soil
435 organic carbon (SOC)-derived CO₂ sequestration and the sum of direct and indirect N₂O emissions,
436 expressed on a CO₂-equivalent (CO₂equ) basis. A negative GHG balance indicates that the cropping
437 system acts as a net sink of GHGs (i.e., net CO₂ removal). This approach allows for integrating changes
438 in soil carbon storage with gaseous emissions to provide a comprehensive measure of the system's
439 overall climate performance.

440

441 **3. Results & Discussion**

442 **3.1. Model Performance**

443 [Table 1](#) summarises the predictive performance of the three tree-based models evaluated in this study
444 and shows that all models achieved generally acceptable accuracy across the target variables. However,
445 XGBoost and LightGBM consistently outperformed CatBoost, exhibiting higher coefficients of
446 determination and lower error metrics. Although XGBoost and LightGBM achieved very similar



447 predictive performance across all target variables, XGBoost was selected as the final model due to its
 448 substantially faster inference time. On average, XGBoost required approximately three minutes to
 449 generate predictions for all four variables, whereas LightGBM required nearly one hour to produce the
 450 same outputs under identical computational conditions. This difference in inference efficiency is critical
 451 given the scale of simulations in this study involving millions of management combinations and the
 452 need for timely generation of management scenario outcomes. The markedly lower inference cost
 453 makes XGBoost cheaper to deploy at scale and thus more suitable as a surrogate model within
 454 computationally intensive optimisation loops.

455
 456
 457

Table 1. Performance of CatBoost, XGBoost, and LightGBM across possibility and actual spaces

Variable	Model	R ² (possibility)	R ² (actual)	RMSE (possibility)	RMSE (actual)
N ₂ O (kg N ha ⁻¹)	CatBoost	0.73	0.63	0.59	0.39
	XGBoost	0.81	0.70	0.50	0.35
	LightGBM	0.81	0.71	0.49	0.35
NO ₃ ⁻ (kg N ha ⁻¹)	CatBoost	0.75	0.69	23.83	12.67
	XGBoost	0.84	0.80	19.22	10.20
	LightGBM	0.83	0.78	19.66	10.53
Yield (kg DM ha ⁻¹)	CatBoost	0.91	0.90	723.87	696.89
	XGBoost	0.93	0.92	626.70	594.68
	LightGBM	0.95	0.95	543.86	495.85
SOC (kg C ha ⁻¹)	CatBoost	0.79	0.66	359.94	341.33
	XGBoost	0.86	0.76	288.72	286.76
	LightGBM	0.86	0.74	293.30	299.39

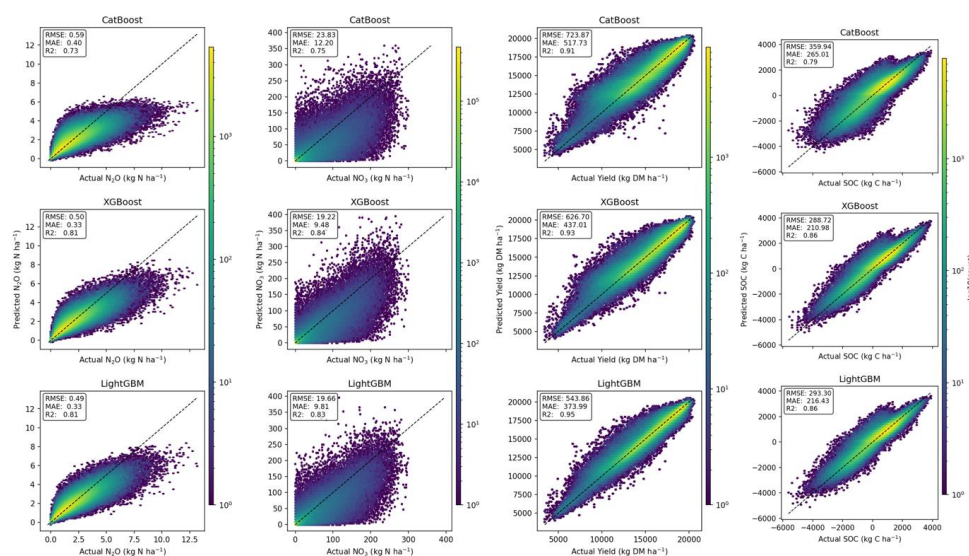
458 Note: “Possibility space” refers to model evaluation on the synthetic dataset, and “actual space” refers
 459 to evaluation on an independent dataset that reflects real-world conditions.

460

461 [Figure 2 \(A & B\)](#) complements the quantitative metrics reported in [Table 1](#) by providing a diagnostic
 462 comparison of predicted versus simulated values for all target variables across the three tree-based
 463 models. The scatter density plots show a strong alignment along the 1:1 line for yield and soil organic
 464 carbon, indicating stable predictions across the full value range. For nitrous oxide emissions and nitrate
 465 leaching, a wider dispersion is observed, particularly at higher values, reflecting the greater intrinsic
 466 variability of these processes and the presence of episodic extremes. Nevertheless, no pronounced
 467 systematic over or underestimation is evident, and prediction errors remain broadly symmetric.

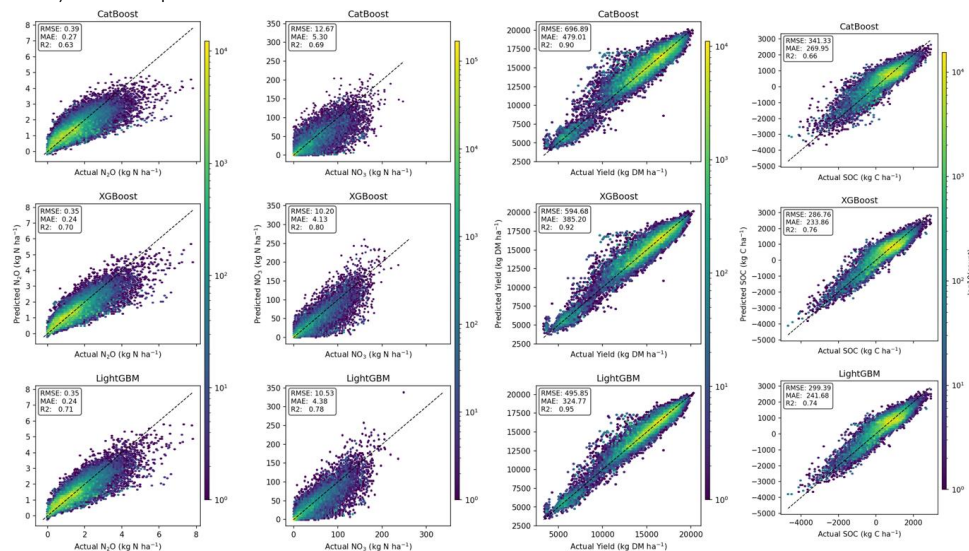
468

469 A) Possibility Space



470
471

B) Actual Space



472
473

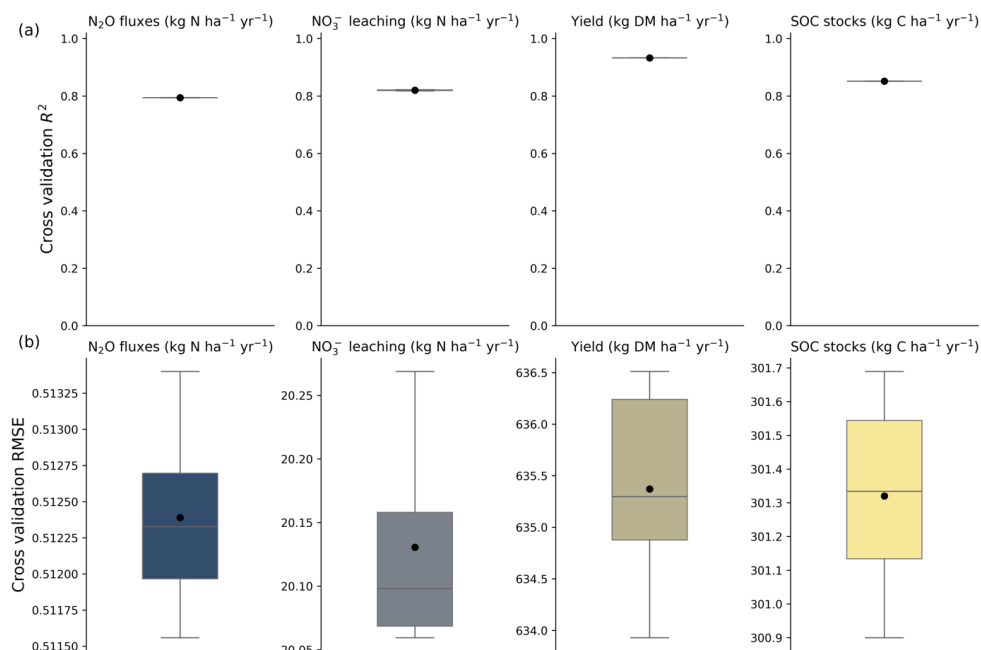
Figure 2. Performance metrics for CatBoost, XGBoost, and LightGBM across the four predicted variables (N₂O, NO₃⁻, SOC, and yield). Panel A shows RMSE, MAE, and R² in the possibility space, and Panel B shows the corresponding metrics in the actual space.

474
475
476
477
478
479
480
481
482
483
484
485

Figure 3 presents the cross-validation results, indicating an extremely narrow range between the mean and standard deviation of the cross-validated R² values. This shows a consistent performance across folds, suggesting minimal overfitting and strong generalization capacity. When model predictions on national data were compared to Denmark national yield data for Winter Wheat from Statistics Denmark (<https://www.dst.dk>), the fully trained XGBoost model achieved a R² of 0.77 against the national yield data as shown in Figure S.1, indicating strong agreement between model predictions and independent observations. This level of performance demonstrates that the model captures key biophysical processes and its potential applicability for large-scale agroecosystem assessments.



486
487
488
489



490
491
492
493
494
495

Figure 3. Stability of R² across 5-fold cross validation for N₂O, NO₃⁻, yield, and SOC. It illustrates the variability and consistency of model performance within each fold, providing insight into the robustness and generalizability of the selected model across different subsets of the data. We highlight how in (b) the variability is artificial due to the extremely small variation (e.g., 0.51150 and 0.51325 kg N-N₂O ha⁻¹ yr⁻¹).

496
497
498
499
500
501
502
503
504
505
506
507
508
509
510
511
512
513
514
515

An important highlight in the development of mLDNDC is the importance of incorporating seasonal climate descriptors and detailed soil variables into the feature set. Although the surrogate model produces annual predictions, several of the target variables, particularly nitrous oxide emissions, operate at much finer temporal scales and are strongly shaped by short term environmental fluctuations and episodic “hot moments”. Without information that captures seasonal temperature and precipitation dynamics, as well as conditions immediately surrounding nutrient applications, the model was unable to fully represent the drivers of these sub-annual processes. Early versions of the model relied primarily on soil texture classes alongside a limited selection of soil physical and chemical properties. Under this simplified representation, the surrogate achieved moderate performance, with R² values of approximately 0.64 for N₂O emissions, 0.70 for nitrate leaching, 0.88 for yield, and 0.65 for soil organic carbon. When the feature set was expanded to include seasonal precipitation and temperature patterns, climatic conditions during the crop growth period, and rainfall events before and after fertiliser and manure applications, along with key soil variables such as available carbon, soil nitrogen concentration, field capacity, wilting point, bulk density, and pH; the performance improved substantially. The corresponding R² values increased to 0.81, 0.84, 0.93, and 0.86 for N₂O, NO₃⁻, yield, and SOC respectively. These improvements reinforce the well-established understanding that soil nitrogen availability, soil carbon content, moisture status, aeration, temperature, and pH jointly regulate nitrogen cycling processes and N₂O production. This has been consistently reported in the literature, including (C. Wang et al., 2021), that highlight the strong direct and indirect influence of soil carbon, soil nitrogen concentration, soil moisture, temperature, and pH on N₂O emissions.



516 Another important finding to consider with respect to feature engineering is that response variable
517 transformation to deal with heteroscedasticity improved model performance. For gradient-boosted
518 decision trees, stabilising the distribution of the response variable enhances model performance
519 because the underlying optimisation uses a stage-wise additive framework that is sensitive to the scale
520 and variance of residuals. (Friedman, 2001), who introduced gradient boosting, emphasised that
521 reducing skewness and variance asymmetry in the target variable improves the convergence and
522 stability of boosted models. (Kuhn & Johnson, 2013) similarly showed that transformations improve
523 predictive accuracy by reducing the influence of extreme values and enabling tree-based models to
524 make more effective splits. A more recent study by (Karwowska et al., 2025) show that data
525 transformation can address data challenges in machine learning tasks.

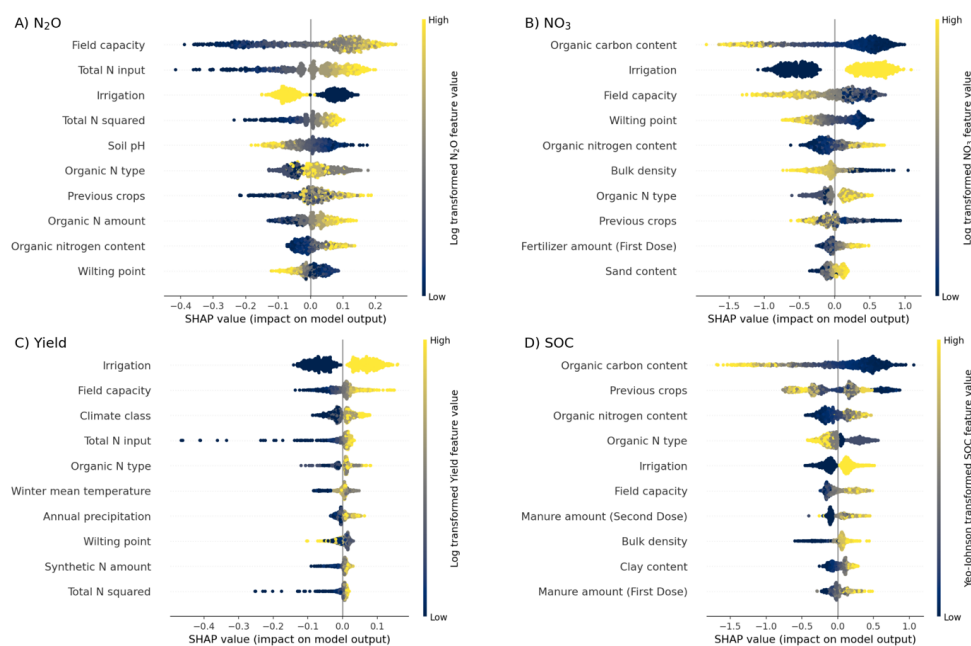
526 The enhanced performance of mLDNDC after integrating these variables demonstrates that surrogate
527 models can successfully capture the sensitivity of nitrogen and carbon processes to dynamic
528 environmental conditions when provided with appropriately engineered features.

529 It is also important to note that neural networks were explored during the early stages of model
530 development, but their performance was consistently poor across both the training and validation
531 phases making them excluded from this study. This behaviour is consistent with observations in the
532 broader machine learning literature, where conventional feed forward neural networks often struggle
533 with tabular datasets, particularly when the underlying relationships are non-sequential and dominated
534 by heterogeneous feature interactions rather than spatial or temporal dependency structures (Borisov
535 et al., 2024; Shwartz-Ziv & Armon, 2022). Deep learning architectures such as Long Short-Term Memory
536 network (LSTM), Gated Recurrent Unit (GRU), and Transformers typically offer advantages when
537 modelling sequential or high dimensional unstructured data, which was not the case in this study. In
538 contrast, tree-based ensemble methods such as XGBoost are well known for their superior
539 performance on structured agricultural and environmental datasets, which likely explains their
540 substantial advantage in the present application.

541 3.2. Model Interpretation Using SHAP

542 To interpret the associations and interactions underlying the model predictions for each target variable,
543 we computed SHAP values for samples drawn randomly from synthetic observations (Figure 4). The
544 SHAP summary plots show the relative importance, intensity of influence, and model response on
545 feature magnitude by showing the distribution of SHAP values for each feature across all samples. We
546 interpret these results primarily as model-based associations inferred from the data, not as causal
547 mechanisms. However, consistent and agronomically plausible SHAP patterns can be suggestive of
548 underlying causal relationships and thus serve as a structured basis for formulating causal hypotheses.

549
550



551
552

553 **Figure 4. SHapley Additive exPlanations (SHAP) values of the four predicted variables (N₂O, NO₃⁻, Crop Yield & SOC).**
554 **The vertical position of a feature reflects its overall importance, while the horizontal spread and colour show the**
555 **direction and strength of its effect across all observations.**

556

557 Below we highlight the five key drivers per SHAP analysis for each one of the target variables:

558

559 **N₂O.** The five most influential predictors of N₂O emissions are field capacity, total N input (represented
560 by both linear and squared terms to reflect the nonlinear increase in emissions at higher nitrogen
561 application levels), irrigation, soil pH, and type of organic (e.g., slurry, farmyard manure).

562

563 Soils with high water holding capacity tend to have higher predicted N₂O emissions, as indicated by
564 positive SHAP values. This is consistent with the central role of soil moisture in regulating nitrification
565 and denitrification via controlling soil oxygen diffusion and redox conditions. N₂O fluxes increase as
566 water-filled pore space approaches field capacity (Ciarlo et al., 2006; Diba et al., 2011). At this point,
567 anaerobic microsites become more frequent but complete reduction to N₂ is still limited (Ciarlo et al.,
568 2006). Total N input and its squared term show that higher fertiliser N rates significantly increase
569 predicted N₂O emissions. The squared term captures the well-known non-linear, accelerating response
570 of N₂O emissions to N addition. Global meta-analyses report that N₂O emissions rise disproportionately
571 at high N rates, with emission factors increasing when fertiliser inputs exceed crop demand (Maaz et
572 al., 2021; Shcherbak et al., 2014). Therefore, the model behaviour aligns with the established
573 understanding that efficient N management is critical for N₂O mitigation.

574

575 Interestingly, Irrigation, encoded as a binary factor, shows that irrigated sites (high feature value) tend
576 to have negative SHAP values, implying lower predicted N₂O emissions than non-irrigated sites. Many
577 experiments report increased N₂O under excessive wetting, especially when soils remain close to
578 saturation (Huang & Gerber, 2015). However, there is also evidence that controlled irrigation around
579 field capacity can suppress denitrification and N₂O emissions compared to extremes of very dry or very
580 wet conditions, particularly in drip-irrigated systems where water is applied in small doses (Zhang et al.,
581 2024).

582

583 Soil pH is strongly negatively associated with N₂O emissions: higher pH values produce negative SHAP
584 values, indicating reduced predicted emissions. This aligns with experimental and meta-analytic
585 evidence that liming acidic soils enhances the activity of N₂O reductase and shifts denitrification end-



582 products from N_2O to N_2 , reducing total N_2O emissions (Hénault et al., 2019; Y. Wang et al., 2021;
583 Žurovec et al., 2021).

584 Organic N type, a categorical variable describing the form of organic fertiliser, also ranks among the
585 leading predictors. Some organic N types are associated with positive SHAP values (higher N_2O), while
586 others are associated with negative SHAP values. This is in line with comparative studies that show
587 different fertiliser forms and C:N ratios alter N turnover and gaseous losses (Yao et al., 2022).

588 **NO_3^- leaching.** The dominant predictors of NO_3^- leaching are organic carbon content, irrigation, field
589 capacity, wilting point, and organic N content. Low soil organic carbon content corresponds to positive
590 SHAP values and higher predicted NO_3^- leaching losses, whereas high organic carbon content tends to
591 reduce leaching. This agrees with experimental studies showing that increased soil organic matter can
592 enhance microbial immobilisation of nitrate and improve soil structure, thereby reducing leaching
593 losses (Malcolm et al., 2019).

594 The capacity to irrigate is strongly positively associated with NO_3^- leaching, with irrigated fields showing
595 large positive SHAP values. Global meta-analyses of irrigated systems demonstrate that nitrate leaching
596 risk is inherently high when water inputs exceed crop demand, and that both irrigation amount and
597 timing are key determinants of leaching losses (Quemada et al., 2013). Thus, the model therefore
598 captures the trade-off between yield benefits of irrigation and increased risk of leaching.

599 Both field capacity and wilting point, clearly demonstrates the effects of soil water holding properties
600 and texture. Soils with low field capacity and low wilting point (i.e., coarse, free-draining soils) have
601 positive SHAP values and higher predicted leaching. In contrast, finer textured soils with greater water
602 holding ability tend to have lower NO_3^- losses. This is consistent with field and meta-analytic studies
603 that link high leaching risks to sandy or structurally weak soils with poor water and nutrient retention,
604 especially in areas of high rainfall or irrigation (Pacheco & Sumreen Hina, 2024; Schuster et al., 2022).

605 Organic N content, representing the amount of organic N in the soil, is positively associated with NO_3^-
606 leaching. High organic N content increases the pool of mineralisable N, which under moist conditions
607 and sufficient aeration leads to increased nitrate formation and a larger leachable pool. Recent work
608 has shown that soil C and N contents, and their ratios, are pivotal in regulating mineralisation,
609 immobilisation, and nitrate availability (Kuśmierz et al., 2023; Ma et al., 2018).

610 **Winter wheat yield.** The five leading predictors of yield are irrigation, field capacity, climate class, total
611 N input (including its squared term), and organic N type. Irrigation has large positive SHAP values when
612 the field is irrigated, indicating substantial yield benefits relative to non-irrigated conditions. Meta-
613 analyses of wheat production consistently show that well managed irrigation increases grain yield and
614 water productivity compared to rainfed systems, especially in water-limited environments. Reported
615 yield gains range from 10–30 percent depending on deficit level and environment (Li et al., 2022; Ren
616 et al., 2025; Zhou et al., 2022). Therefore, the model performance is fully aligned with empirical
617 evidence. Field capacity emerges as a critical soil property, with higher field capacity associated with
618 positive SHAP values and higher predicted yields. Soils with greater plant-available water storage buffer
619 crops against intra-seasonal drought, thereby stabilising and increasing yield. Recent analyses of long-
620 term experiments and meta-studies on soil water storage (Lessmann et al., 2022; Slessarev et al., 2022)
621 confirm that improved soil structure and water retention are strongly linked to wheat yield and stability.
622 Climate class, which summarises the prevailing temperature and precipitation regime through aridity
623 index classification, is also highly influential. This mirrors established knowledge that winter wheat
624 yields in northern Europe are strongly constrained by temperature and water availability during critical
625 growth stages, and that inter-annual climate variability is a major driver of yield variation.

626 Total N input, represented by both linear and squared terms, shows the expected yield response curve
627 as moderate N rates increase predicted yield (positive SHAP values) while very high rates are associated
628 with neutral or even negative contributions once the squared term dominates. Trials of yield response
629 in Scandinavia including Denmark demonstrate that grain yield increases with N up to an economically
630 optimal rate. Beyond this rate, additional N has little effect on yield but increases environmental losses
631 (Styczen et al., 2020; Vogeler et al., 2022). The model captures this diminishing return and embeds it



632 through the quadratic N term. In the case of Organic N type, the influence on the prediction is based
633 on the different C:N ratios of the different organic manure applied.

634 **Changes in soil organic carbon.** The five most important predictors of SOC changes are initial organic
635 carbon content, previous crops, organic nitrogen content, organic N type, and irrigation. The SHAP
636 pattern for organic carbon content shows that soils with low initial SOC tend to have positive SHAP
637 values, indicating a greater predicted SOC gain. In contrast, soils with high initial SOC often have
638 negative contributions. This is consistent with recent global analyses demonstrating that SOC-poor soils
639 generally exhibit higher sequestration potential and gain carbon more readily in response to improved
640 management than SOC-rich soils, which are closer to saturation (Lessmann et al., 2022; Slessarev et al.,
641 2022).

642 Previous crops, representing the two crops grown before winter wheat, have a strong effect on SOC.
643 Long-term rotation experiments and recent global syntheses show that diversified rotations especially
644 with legumes enhance SOC stocks and soil health relative to continuous cereal systems (Al-Musawi et
645 al., 2025; Yang et al., 2024).

646 Organic nitrogen content, which reflects cumulative organic inputs and soil organic N, contributes
647 positively to SOC predictions when high. This is consistent with evidence that increased organic inputs
648 from manure, crop residues, or combined mineral-organic fertilisation increase soil C stocks while also
649 supporting higher yields (Ma et al., 2018). The influence of organic N type is based on the C:N ratios of
650 the applied manure.

651 Finally, there is positive relationship between irrigation and SOC. Irrigated sites showed higher
652 predicted SOC than non-irrigated sites. Meta-analyses of irrigated agriculture indicate that irrigation
653 generally increases SOC stocks, especially in surface soils, by promoting greater biomass production
654 and residue return. However, the magnitude of this effect depends on climate and management
655 practices (Antón et al., 2022; Emde et al., 2021; Sun et al., 2024). The SHAP result suggests that, in the
656 Danish context considered here, irrigation contributes to higher SOC through enhanced primary
657 productivity and associated organic input.

658 3.2. Baseline-to-Optimised Differences at the National Scale

659 3.2.1. Changes in N₂O Emissions, NO₃⁻ Leaching, Grain Yield, and SOC

660 **Figure 5a** illustrates the spatial distribution of the optimisation benefits for N₂O emissions across
661 Denmark. Because the optimisation objective for both N₂O and NO₃⁻ is minimisation, the percentage
662 changes shown on the map indicate the extent to which emissions can be reduced relative to the
663 baseline (**Figure S.6**). Depending on their location within the 10 × 10 km grid, many grid cells across the
664 country show reductions ranging from approximately 15 percent to more than 35 percent. **Figure 5e**'s
665 national-level summary **further** confirms this pattern. The N₂O emission bar indicates that an average
666 reduction of about 26 percent can be achieved through optimised cropping system management.

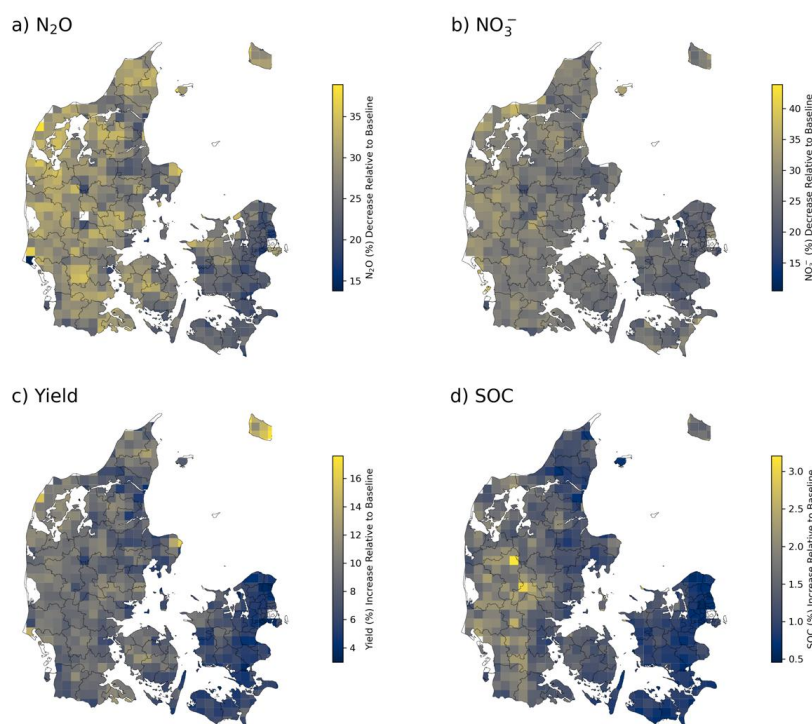
667 Similarly, **Figure 5b** shows that nitrate leaching can also be substantially reduced. In some grid cells,
668 reductions reach up to about 40 percent, while most areas show improvements of roughly 30 percent.
669 The national aggregation in **Figure 5e** indicates an average reduction of approximately 27 percent.
670 These reductions in both N₂O emissions and NO₃⁻ leaching is achieved without compromising yield or
671 soil organic carbon, demonstrating the potential for environmentally beneficial optimisation of Danish
672 cropping systems.

673 The optimization objective for yield and SOC is maximisation. The spatial pattern in **Figure 5c** reveals
674 that crop yield can increase by up to 16 percent in some grid cells, with most areas showing
675 improvements of around 10 percent. The national average, shown in **Figure 5e**, is approximately 8
676 percent. Importantly, these gains are achieved without increasing N₂O emissions or NO₃⁻ leaching,
677 indicating that higher productivity can coexist with reduced environmental impacts.

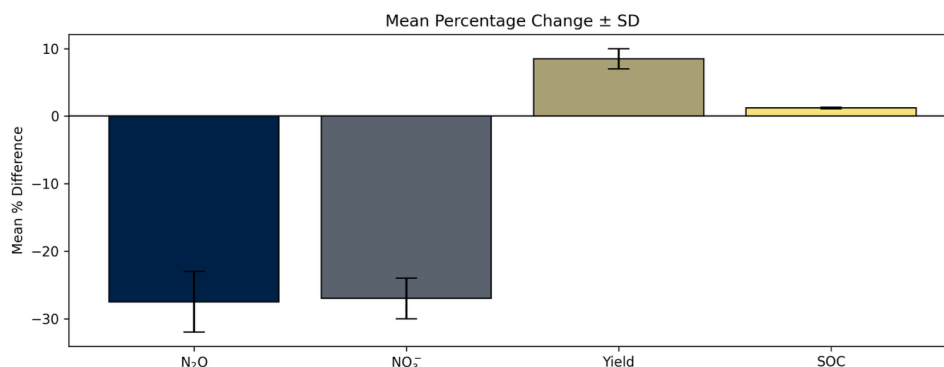
678 SOC shows a similar pattern of improvement. As illustrated in **Figure 5d**, SOC can be increased by up to
679 3 percent in some areas, with most regions showing increases of around 2 percent. The national mean,
680 as reflected in **Figure 5e**, is about 1 percent, which is close to the noise level of measurement and should
681 be interpreted as marginal improvements rather than large changes. Although this magnitude is smaller



682 than the yield response, it represents a meaningful improvement given the slow dynamics of soil carbon
683 accumulation.
684 These results demonstrate that optimised management strategies can simultaneously reduce N₂O
685 emissions and NO₃⁻ leaching while enhancing crop yield and SOC. It further highlights the potential for
686 integrated, multi-objective optimisation to support both environmental and agronomic goals within
687 Danish cropping systems. The percentage of specific management changes in each 10 x 10km grid are
688 shown in (Figure S.5)



689
690 e) National



691
692 Figure 5. Panels (a–d) show the percentage difference between optimised management and the baseline scenario
693 over the 10-year period from 2011 to 2020, aggregated to a 10 × 10 km grid, with decreases shown for N₂O
694 emissions and NO₃⁻ leaching and increases shown for yield and soil organic carbon. Panel (e) presents the
695 corresponding mean percentage change at the national scale.



696

697 3.2.2 Nitrogen and Greenhouse Gas Performance Indicators

698 A) Nitrogen Use Efficiency

699 In addition to the environmental and productivity gains identified in the multi-objective optimisation,
700 the results also demonstrate clear improvements in nitrogen use efficiency (NUE) defined as follows:

701

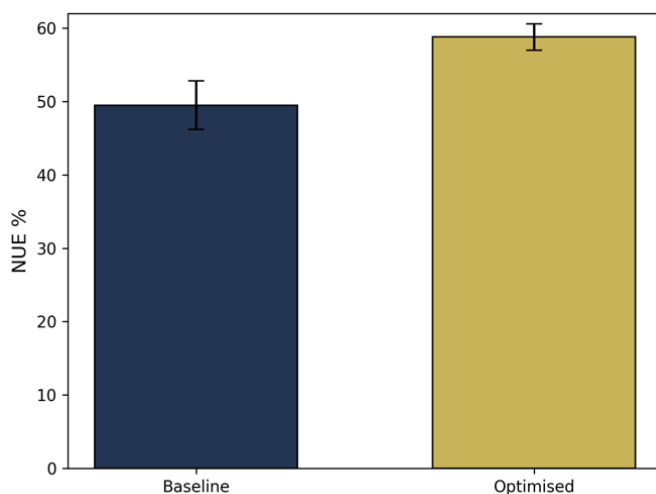
$$702 \quad \text{NUE} = \frac{Y}{FN} * 100$$

703 where Y is the crop yield (kg N ha^{-1}), and FN is the amount of fertiliser nitrogen applied (kg N ha^{-1}).

704

705 As shown in [Figure 6](#), optimised management strategies increase NUE across most regions of Denmark,
706 with national level gains averaging approximately 10 percent relative to the baseline. This indicates that
707 the optimised cropping systems can produce more yield per unit of nitrogen applied, reflecting more
708 efficient nitrogen utilisation without increasing N_2O emissions or nitrate leaching. Such improvements
709 in NUE align with the broader goals of enhancing nitrogen productivity while reducing surplus nitrogen
710 in agricultural landscapes.

711



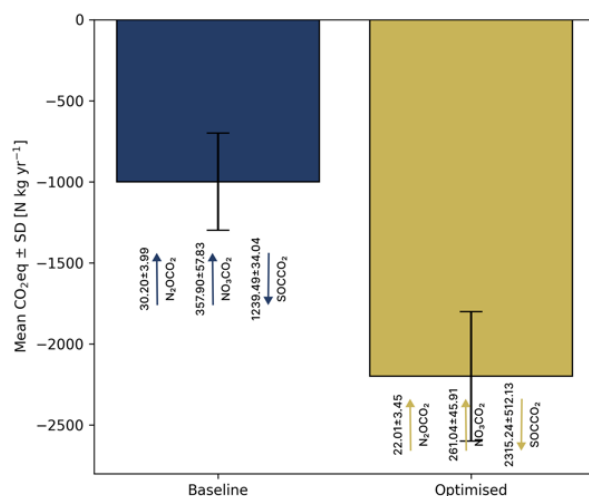
712

713 **Figure 6. Nitrogen Use Efficiency of baseline and optimized management over 10 years (2011-2020).**

714

715 B) Soil Net GHG Balance

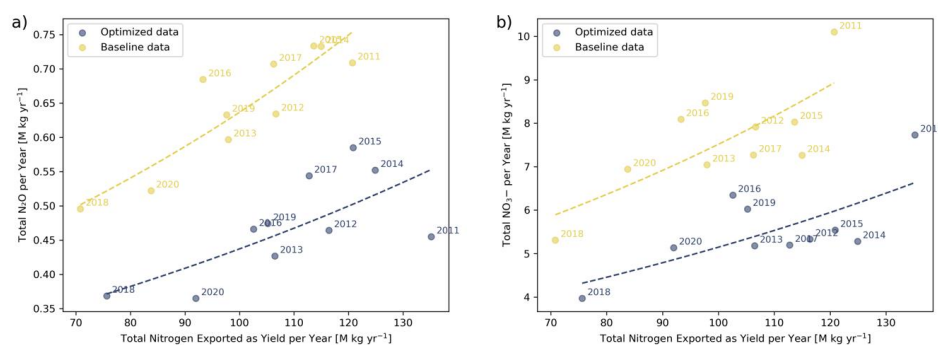
716 [Figure 7](#) compares the CO_2 -equivalent ($\text{CO}_2\text{-eq}$) soil-net GHG balance of the baseline and optimised
717 management scenarios over the 10-year period 2011–2020. The optimised scenario exhibits a
718 substantially more negative $\text{CO}_2\text{-eq}$ value than the baseline, indicating greater net climate benefits
719 through enhanced carbon sequestration and reduced emissions. Moreover, the wider negative range
720 shown by the error bar suggests that optimisation improves mitigation potential consistently across
721 spatial and inter-annual variability over the 10-year period. Overall, the results demonstrate that
722 systematically optimising management practices can meaningfully strengthen the climate mitigation
723 capacity of Danish cropping systems.



724
 725 **Figure 7.** Soil-net GHG balance ($\text{Mg CO}_2\text{-eq ha}^{-1} \text{yr}^{-1}$) under baseline and optimised management scenarios, averaged
 726 over the 10-year period 2011–2020; negative values indicate greater net climate-mitigation potential.
 727

728 **C) Total N_2O and NO_3^- per Nitrogen Yield**

729 **Figure 8** illustrates the relationship between total nitrogen exported as yield and the corresponding
 730 annual N_2O emissions and NO_3^- losses for both the baseline and optimised scenarios. The optimised
 731 management consistently shifts observations upward and to the right, indicating higher nitrogen export
 732 through increased yield while simultaneously reducing N_2O emissions and NO_3^- leaching relative to the
 733 baseline. This pattern shows that the optimised system achieves greater nitrogen productivity without
 734 incurring additional gaseous or leaching losses, demonstrating improved overall nitrogen stewardship
 735 in Danish cropping systems.
 736



737
 738 **Figure 8.** Total nitrogen exported as yield per year compared with (a) total N_2O emissions per year and (b) total NO_3^-
 739 leaching per year for baseline and optimised management.
 740

741
 742 **4. Conclusion**

743 The development of the surrogate model mLDNDC was motivated by the need for a computationally
 744 efficient alternative to full process-based simulations when conducting multi-objective optimisation at
 745 scale. While process-based models provide detailed mechanistic representations of agroecosystem
 746 dynamics, they remain computationally demanding when thousands of management scenarios must



747 be evaluated repeatedly. mLDNDC preserves the core behavioural response of the LandscapeDNDC
748 model while reducing runtime by several orders of magnitude. This computational gain enables
749 optimisation across large spatial domains, allows the evaluation of a far broader range of management
750 combinations, and supports systematic exploration of trade-offs and synergies among multiple
751 environmental and productivity outcomes.
752 Importantly, the surrogate model does not replace the process-based model but supplements it by
753 making national-scale optimisation feasible in practice. As a data-driven approximation, the surrogate
754 can reliably predict only the outputs and objectives included in its training data. If additional objectives,
755 such as new biogeochemical indicators or management goals, are introduced, the surrogate must be
756 retrained using corresponding simulations from the process-based model. In contrast, process-based
757 models explicitly simulate the underlying biophysical processes governing system behaviour. They
758 embed mathematical representations of physical, chemical, and biological processes, including soil
759 water dynamics, plant growth, nutrient cycling, and greenhouse gas fluxes. As a result, they generate
760 intermediate state variables, such as microbial activity or nitrification and denitrification rates, that
761 provide explanatory insight into system functioning beyond final outputs like yield or emissions (Kim et
762 al., 2025). This fundamental difference in model design leads to distinct but complementary roles.
763 Process-based models offer broad scope, interpretability, and flexibility, whereas surrogate models
764 provide speed and scalability but limited process transparency.
765 This study was designed as a multi-objective optimisation experiment to assess whether agronomic
766 management can simultaneously sustain high crop productivity while delivering substantial
767 environmental co-benefits at national scale. The underlying premise is that sustainable arable systems
768 must balance yield with reductions in greenhouse gas emissions, nitrogen losses, and soil degradation,
769 rather than optimising any single outcome in isolation. A single-objective formulation, such as yield
770 maximisation alone, would have obscured potential win-win solutions and provided limited insight into
771 trade-offs or synergies among productivity, nitrogen use efficiency, and environmental performance
772 relative to current practice in Denmark.
773 To the best of current knowledge, no previous study in Denmark has applied a standard multi-objective
774 optimisation framework to crop management using a surrogate-based approach capable of evaluating
775 thousands of spatially explicit management combinations. In contrast to studies based on a limited set
776 of predefined scenarios, this work demonstrates that more balanced outcomes are achievable. The
777 optimisation identified management strategies that reduced N₂O emissions by 27.5 ± 4.5 percent and
778 NO₃⁻ leaching by 27 ± 3.0 percent, while simultaneously increasing grain yield by 8.5 ± 1.5 percent and
779 soil organic carbon stocks by 1.2 ± 0.1 percent, alongside a 10 ± 2 percent improvement in nitrogen use
780 efficiency. These improvements were achieved without increasing total fertiliser inputs. Instead, gains
781 arose from reallocating mineral and organic nitrogen, adjusting incorporation depth, and optimising
782 residue management, catch-crop use, and irrigation practices. Collectively, these changes shifted the
783 system towards a substantially lower net greenhouse gas balance relative to current practices.
784 Despite its strengths, the surrogate modelling approach has limitations. Model performance depends
785 on the breadth and quality of the synthetic training data generated from the process-based model, and
786 gaps in the simulation design may reduce accuracy when the surrogate extrapolates beyond the
787 training domain. In addition, the optimisation framework does not currently account for economic
788 costs, labour availability, or machinery constraints, which are important determinants of real-world
789 adoption. Incorporating these factors in future work would improve the practical relevance of the
790 results. Furthermore, while the present study focuses on winter wheat systems, extending the
791 surrogate framework to full crop rotations would provide a more comprehensive representation of
792 Danish arable agriculture.
793 The development of mLDNDC also highlighted the importance of including detailed seasonal climate
794 information and soil variables to faithfully replicate the behaviour of the full process-based model. The
795 marked improvement in surrogate performance following the inclusion of these variables demonstrates
796 that careful feature engineering is essential when using machine learning to emulate complex
797 biogeochemical processes.



798 Collectively, the results show that mLDNDC is an effective and computationally efficient tool for
799 exploring management scenarios and supporting multi-objective optimisation at national scale. When
800 coupled with appropriate decision-making frameworks, it offers substantial potential to inform policy
801 development, advisory services, and strategic planning aimed at balancing agricultural productivity with
802 environmental sustainability.
803 Several avenues for future research emerge from this work. Linking mLDNDC with socioeconomic and
804 land-use models would enable assessment of national-scale policy interventions, including nitrogen
805 quotas, carbon pricing mechanisms, fertiliser price changes, and incentives for manure redistribution.
806 The computational efficiency of the surrogate makes it well suited for integration with economic
807 optimisation or agent-based modelling frameworks to explore behavioural responses across farming
808 systems. In addition, incorporating climate change scenarios would allow evaluation of the robustness
809 of optimised management strategies under projected changes in temperature and precipitation, which
810 is essential for designing resilient cropping systems.
811 Finally, the strong spatial heterogeneity observed in optimisation outcomes highlights the need for
812 regionalised advisory tools and policy support. mLDNDC could serve as the computational core of
813 interactive decision-support systems that provide grid-specific recommendations tailored to local soils,
814 climate, and management histories. Overall, the methodological framework developed in this study
815 provides a scalable and robust foundation for next-generation agricultural assessment and
816 optimisation. With further integration of socioeconomic factors and climate projections, mLDNDC has
817 the potential to support Denmark's transition toward climate-smart and resource-efficient agricultural
818 systems.
819
820
821
822



823 **Acknowledgement**

824 This study was supported by the Pioneer Center for Research in Sustainable Agricultural Futures (Land-
825 CRAFT), DNR grant number P2, Aarhus University, Denmark. This research has been funded by the
826 SmartField initiative (supported by Novo Nordisk Foundation under grant number NNF24SA0091172).
827 It has also been partially supported by DeIC National HPC (Interactive & Throughput) (DeiC-AU-N1-
828 2024070 & DeiC-AU-N1-2024071).

829

830 **Code and data availability**

831 The code used for training all machine learning models presented in this manuscript are publicly
832 available on Zenodo at <https://doi.org/10.5281/zenodo.18278474> (Aderere et al., 2026a). The
833 datasets are publicly available on Zenodo at <https://doi.org/10.5281/zenodo.18573225> (Aderere et
834 al., 2026b)

835

836

837 **Author Contribution**

838 M.O.A and J.R. conceived and designed the study, prepared model input data, performed the analysis.
839 M.O.A and J.R. wrote the first draft, while all co-authors (E.H., L.L., J.S., and K.B.B.) have contributed to
840 improving the manuscript.

841

842 **Competing Interests**

843 The contact author has declared that none of the authors has any competing interests.

844

845

846 **References**

- 847 Abdu, A., Laekemariam, F., Gidago, G., Kebede, A., & Getaneh, L. (2023). Variability analysis of soil
848 properties, mapping, and crop test responses in Southern Ethiopia. *Heliyon*, *9*(3), e14013.
849 <https://doi.org/10.1016/J.HELIYON.2023.E14013>
- 850 Aderere, M. O., Haas, E., Liu, L., Serra, J., Kraus, D., Butterbach-Bahl, K., & Rahimi, J. (2026a).
851 *mLDNDCv1.0: A Machine Learning-based Surrogate of LandscapeDNDC for Optimising*
852 *Cropping Systems in Denmark*. Zenodo. <https://doi.org/10.5281/zenodo.18278475>
- 853 Aderere, M. O., Haas, E., Liu, L., Serra, J., Kraus, D., Butterbach-Bahl, K., & Rahimi, J. (2026b).
854 *mLDNDCv1.0: A Machine Learning-based Surrogate of LandscapeDNDC for Optimising*
855 *Cropping Systems in Denmark [Dataset]*. Zenodo.
856 <https://doi.org/10.5281/zenodo.18573226>
- 857 Aderere, M. O., Haas, E., Smerald, A., Blicher-Mathiesen, G., Butterbach-Bahl, K., & Rahimi, J.
858 (2025). The environmental trade-off of fertiliser, residue and catch crop management in
859 Danish cropping systems. *Agricultural Systems*, *229*, 104433.
860 <https://doi.org/10.1016/J.AGSY.2025.104433>
- 861 Aderere, M. O., Srivastava, A. K., Butterbach-Bahl, K., & Rahimi, J. (2025). Integrating machine
862 learning with agroecosystem modelling: Current state and future challenges. *European*
863 *Journal of Agronomy*, *168*, 127610. <https://doi.org/10.1016/J.EJA.2025.127610>
- 864 Akiba, T., Sano, S., Yanase, T., Ohta, T., & Koyama, M. (2019). Optuna: A Next-generation
865 Hyperparameter Optimization Framework. *Knowledge Discovery and Data Mining*, 2623–
866 2631. <https://doi.org/10.1145/3292500.3330701>
- 867 Al-Musawi, Z. K., Vona, V., & Kulmány, I. M. (2025). Utilizing Different Crop Rotation Systems for
868 Agricultural and Environmental Sustainability: A Review. *Agronomy 2025*, Vol. 15, Page 1966,
869 *15*(8), 1966. <https://doi.org/10.3390/AGRONOMY15081966>
- 870 Antón, R., Derrien, D., Urmeneta, H., van der Heijden, G., Enrique, A., & Virto, I. (2022). Organic
871 Carbon Storage and Dynamics as Affected by the Adoption of Irrigation in a Cultivated
872 Calcareous Mediterranean Soil. *Frontiers in Soil Science*, *2*, 831775.
873 <https://doi.org/10.3389/FSOIL.2022.831775/FULL>



- 874 Attia, A., Govind, A., Qureshi, A. S., Feike, T., Rizk, M. S., Shabana, M. M. A., & Kheir, A. M. S. (2022).
875 Coupling Process-Based Models and Machine Learning Algorithms for Predicting Yield and
876 Evapotranspiration of Maize in Arid Environments. *Water (Switzerland)*, 14(22).
877 <https://doi.org/10.3390/w14223647>
- 878 Baker, R. E., & Anttila-Hughes, J. (2020). Characterizing the contribution of high temperatures to
879 child undernourishment in Sub-Saharan Africa. *Scientific Reports*, 10(1), 1–10.
880 <https://doi.org/10.1038/S41598-020-74942-9>;SUBJMETA
- 881 Barua, S. K., Berg, P., Bruvoll, A., Cederberg, C., Drinkwater, K. F., Eide, A., Eythorsdottir, E.,
882 Guðjónsson, S., Gudmundsson, L. A., Gundersen, P., Hoel, A. H., Jarp, J., Jørgensen, R. B.,
883 Kantanen, J., Kettunen-Præbel, A., Løvendahl, P., Meuwissen, T., Olesen, J. E., Portin, A., ...
884 Stiansen, J. E. (2014). *Climate change and primary industries : Impacts, adaptation and*
885 *mitigation in the Nordic countries*. <https://doi.org/10.6027/TN2014-552>
- 886 Blank, J., & Deb, K. (2020). Pymoo: Multi-Objective Optimization in Python. *IEEE Access*, 8, 89497–
887 89509. <https://doi.org/10.1109/ACCESS.2020.2990567>
- 888 Borisov, V., Leemann, T., Sebler, K., Haug, J., Pawelczyk, M., & Kasneci, G. (2024). Deep Neural
889 Networks and Tabular Data: A Survey. *IEEE Transactions on Neural Networks and Learning*
890 *Systems*, 35(6), 7499–7519. <https://doi.org/10.1109/TNNLS.2022.3229161>
- 891 Chen, T., & Guestrin, C. (2016). XGBoost: A Scalable Tree Boosting System. *Knowledge Discovery*
892 *and Data Mining, 13-17-August-2016*, 785–794. <https://doi.org/10.1145/2939672.2939785>
- 893 Ciarlo, E., Conti, M., Bartoloni, N., & Rubio, G. (2006). The effect of moisture on nitrous oxide
894 emissions from soil and the N₂O/(N₂O+N₂) ratio under laboratory conditions. *Biology and*
895 *Fertility of Soils* 2006 43:6, 43(6), 675–681. <https://doi.org/10.1007/S00374-006-0147-9>
- 896 Dalgaard, T., Hansen, B., Hasler, B., Hertel, O., Hutchings, N. J., Jacobsen, B. H., Jensen, L. S.,
897 Kronvang, B., Olesen, J. E., Schjørring, J. K., Kristensen, I. S., Graversgaard, M., Termansen,
898 M., & Vejre, H. (2014). Policies for agricultural nitrogen management—trends, challenges
899 and prospects for improved efficiency in Denmark. *Environmental Research Letters*, 9(11),
900 115002. <https://doi.org/10.1088/1748-9326/9/11/115002>
- 901 Deb, K., Pratap, A., Agarwal, S., & Meyarivan, T. (2002). A fast and elitist multiobjective genetic
902 algorithm: NSGA-II. *IEEE Transactions on Evolutionary Computation*, 6(2), 182–197.
903 <https://doi.org/10.1109/4235.996017>
- 904 Diba, F., Shimizu, M., & Hatano, R. (2011). Effects of soil aggregate size, moisture content and
905 fertilizer management on nitrous oxide production in a volcanic ash soil. *Soil Science and*
906 *Plant Nutrition*, 57(5), 733–747.
907 <https://doi.org/10.1080/00380768.2011.604767>;REQUESTEDJOURNAL:JOURNAL:TSSP20;P
908 AGE:STRING:ARTICLE/CHAPTER
- 909 Droutsas, I., Challinor, A. J., Deva, C. R., & Wang, E. (2022). Integration of machine learning into
910 process-based modelling to improve simulation of complex crop responses. *In Silico Plants*,
911 4(2), 1–16. <https://doi.org/10.1093/INSILICOPLANTS/DIAC017>
- 912 Emde, D., Hannam, K. D., Most, I., Nelson, L. M., & Jones, M. D. (2021). Soil organic carbon in
913 irrigated agricultural systems: A meta-analysis. *Global Change Biology*, 27(16), 3898.
914 <https://doi.org/10.1111/GCB.15680>
- 915 Friedman, J. H. (2001). Greedy function approximation: A gradient boosting machine.
916 <https://doi.org/10.1214/Aos/1013203451>, 29(5), 1189–1232.
917 <https://doi.org/10.1214/AOS/1013203451>
- 918 Grados, D., Kraus, D., Haas, E., Butterbach-Bahl, K., Olesen, J. E., & Abalos, D. (2024). Common
919 agronomic adaptation strategies to climate change may increase soil greenhouse gas
920 emission in Northern Europe. *Agricultural and Forest Meteorology*, 349, 109966.
921 <https://doi.org/10.1016/J.AGRFORMET.2024.109966>
- 922 Grote, R., Lavoie, A. V., Rambal, S., Staudt, M., Zimmer, I., & Schnitzler, J. P. (2009). Modelling the
923 drought impact on monoterpene fluxes from an evergreen Mediterranean forest canopy.
924 *Oecologia*, 160(2), 213–223. <https://doi.org/10.1007/S00442-009-1298-9>;FIGURES/8



- 925 Haas, E., Carozzi, M., Massad, R. S., Butterbach-Bahl, K., & Scheer, C. (2022). Long term impact of
926 residue management on soil organic carbon stocks and nitrous oxide emissions from
927 European croplands. *Science of The Total Environment*, 836, 154932.
928 <https://doi.org/10.1016/J.SCITOTENV.2022.154932>
- 929 Haas, E., Klatt, S., Fröhlich, A., Kraft, P., Werner, C., Kiese, R., Grote, R., Breuer, L., & Butterbach-
930 Bahl, K. (2013). LandscapeDNDC: A process model for simulation of biosphere-atmosphere-
931 hydrosphere exchange processes at site and regional scale. *Landscape Ecology*, 28(4), 615–
932 636. <https://doi.org/10.1007/S10980-012-9772-X/FIGURES/12>
- 933 Hansen, L. B., Callesen, G. M., Schou, J. S., Filippelli, R., Hasler, B., Lundhede, T., Termansen, M., &
934 Levin, G. (2025). Land use allocation to achieve multiple goals for climate, aquatic
935 environment, and biodiversity: A scenario analysis for Denmark. *Danish Journal of*
936 *Economics*, (SPECIAL ISSUE ON THE GREEN TRANSITION AND THE DANISH ECONOMY), 65–
937 77.
- 938 Hastie, T., Tibshirani, R., & Friedman, J. (2009). *The Elements of Statistical Learning: Data Mining,*
939 *Inference, and Prediction* (Second Edition). Springer.
- 940 Hénault, C., Bourennane, H., Ayzac, A., Ratié, C., Saby, N. P. A., Cohan, J. P., Eglin, T., & Gall, C. Le.
941 (2019). Management of soil pH promotes nitrous oxide reduction and thus mitigates soil
942 emissions of this greenhouse gas. *Scientific Reports 2019 9:1*, 9(1), 20182-.
943 <https://doi.org/10.1038/s41598-019-56694-3>
- 944 Huang, Y., & Gerber, S. (2015). Global soil nitrous oxide emissions in a dynamic carbon-nitrogen
945 model. *Biogeosciences*, 12(21), 6405–6427. <https://doi.org/10.5194/BG-12-6405-2015>
- 946 Jeong, D., Kim, D., Choi, T., & Seo, Y. (2020). A Process-Based Modeling Method for Describing
947 Production Processes of Ship Block Assembly Planning. *Processes 2020, Vol. 8, Page 880,*
948 8(7), 880. <https://doi.org/10.3390/PR8070880>
- 949 Kapoor, S., & Amazon, V. P. (2021). *A Simple and Fast Baseline for Tuning Large XGBoost Models.*
950 <https://arxiv.org/pdf/2111.06924>
- 951 Karwowska, Z., Aasmets, O., Esko, T., Milani, L., Metspalu, A., Metspalu, M., Kosciolk, T., & Org,
952 E. (2025). Effects of data transformation and model selection on feature importance in
953 microbiome classification data. *Microbiome 2024 13:1*, 13(1), 2-.
954 <https://doi.org/10.1186/S40168-024-01996-6>
- 955 Ke, G., Meng, Q., Finley, T., Wang, T., Chen, W., Ma, W., Ye, Q., & Liu, T.-Y. (2017). LightGBM: A
956 Highly Efficient Gradient Boosting Decision Tree. *Neural Information Processing Systems*.
- 957 Kiese, R., Heinzeller, C., Werner, C., Wochele, S., Grote, R., & Butterbach-Bahl, K. (2011).
958 Quantification of nitrate leaching from German forest ecosystems by use of a process
959 oriented biogeochemical model. *Environmental Pollution*, 159(11), 3204–3214.
960 <https://doi.org/10.1016/J.ENVPOL.2011.05.004>
- 961 Kim, Y. W., Cha, Y. K., & Shin, J. (2025). A modular deep learning surrogate model for simulating
962 harmful algal blooms in complex process-based systems. *Water Research*, 285, 124059.
963 <https://doi.org/10.1016/J.WATRES.2025.124059>
- 964 Kollmer, M. (2023). *Carbon sequestration dynamics of agricultural soils: constraining a*
965 *biogeochemical model with long term field measurements*. Faculty of Environment and
966 Natural Resources, Albert-Ludwigs-University Freiburg im Breisgau.
- 967 Kraus, D., Weller, S., Klatt, S., Haas, E., Wassmann, R., Kiese, R., & Butterbach-Bahl, K. (2015). A
968 new LandscapeDNDC biogeochemical module to predict CH₄ and N₂O emissions from
969 lowland rice and upland cropping systems. *Plant and Soil*, 386(1–2), 125–149.
970 <https://doi.org/10.1007/S11104-014-2255-X/FIGURES/8>
- 971 Kraus, D., Weller, S., Klatt, S., Santabárbara, I., Haas, E., Wassmann, R., Werner, C., Kiese, R., &
972 Butterbach-Bahl, K. (2016). How well can we assess impacts of agricultural land management
973 changes on the total greenhouse gas balance (CO₂, CH₄ and N₂O) of tropical rice-cropping
974 systems with a biogeochemical model? *Agriculture, Ecosystems & Environment*, 224, 104–
975 115. <https://doi.org/10.1016/J.AGEE.2016.03.037>



- 976 Kraus, D., Werner, C., Janz, B., Klatt, S., Sander, B. O., Wassmann, R., Kiese, R., & Butterbach-Bahl,
977 K. (2022). Greenhouse Gas Mitigation Potential of Alternate Wetting and Drying for Rice
978 Production at National Scale—A Modeling Case Study for the Philippines. *Journal of*
979 *Geophysical Research: Biogeosciences*, 127(5). <https://doi.org/10.1029/2022JG006848>
980 Kuhn, M., & Johnson, K. (2013). Applied predictive modeling. In *Applied Predictive Modeling*.
981 Springer New York Heidelberg Dordrecht London. [https://doi.org/10.1007/978-1-4614-](https://doi.org/10.1007/978-1-4614-6849-3)
982 6849-3
983 Kuśmierz, S., Skowrońska, M., Tkaczyk, P., Lipiński, W., & Mielniczuk, J. (2023). Soil Organic Carbon
984 and Mineral Nitrogen Contents in Soils as Affected by Their pH, Texture and Fertilization.
985 *Agronomy* 2023, Vol. 13, Page 267, 13(1), 267.
986 <https://doi.org/10.3390/AGRONOMY13010267>
987 Lessmann, M., Ros, G. H., Young, M. D., & de Vries, W. (2022). Global variation in soil carbon
988 sequestration potential through improved cropland management. *Global Change Biology*,
989 28(3), 1162–1177.
990 <https://doi.org/10.1111/GCB.15954>;REQUESTEDJOURNAL:JOURNAL:13652486;JOURNAL:J
991 OURNAL:13652486;WGROU:STRING:PUBLICATION
992 Li, Z., Cui, S., Zhang, Q., Xu, G., Feng, Q., Chen, C., & Li, Y. (2022). Optimizing Wheat Yield, Water,
993 and Nitrogen Use Efficiency With Water and Nitrogen Inputs in China: A Synthesis and Life
994 Cycle Assessment. *Frontiers in Plant Science*, 13, 930484.
995 <https://doi.org/10.3389/FPLS.2022.930484/BIBTEX>
996 Liebermann, R., Breuer, L., Houska, T., Kraus, D., Moser, G., & Kraft, P. (2019). Simulating Long-
997 Term Development of Greenhouse Gas Emissions, Plant Biomass, and Soil Moisture of a
998 Temperate Grassland Ecosystem under Elevated Atmospheric CO₂. *Agronomy* 2020, Vol. 10,
999 Page 50, 10(1), 50. <https://doi.org/10.3390/AGRONOMY10010050>
1000 Lu, D., Ricciuto, D., & Author, C. (2019). *Efficient surrogate modeling methods for large-scale Earth*
1001 *system models based on machine learning techniques*. <https://arxiv.org/pdf/1901.05125>
1002 Lundberg, S. M., & Lee, S.-I. (2017). A Unified Approach to Interpreting Model Predictions.
1003 *Advances in Neural Information Processing Systems*, 30. <https://github.com/slundberg/shap>
1004 Luo, Z., Wang, E., & Bryan, B. (2011). A meta-model for soil carbon stock in agricultural soils Luo
1005 and Wang, *Estimating soil carbon change using meta-model*.
1006 <http://mssanz.org.au/modsim2011>
1007 Ma, J., Kang, F., Cheng, X., & Han, H. (2018). Response of soil organic carbon and nitrogen to
1008 nitrogen deposition in a Larix principis-rupprechtii plantation. *Scientific Reports* 2018 8:1,
1009 8(1), 8638-. <https://doi.org/10.1038/s41598-018-26966-5>
1010 Maaz, T. M., Sapkota, T. B., Eagle, A. J., Kantar, M. B., Bruulsema, T. W., & Majumdar, K. (2021).
1011 Meta-analysis of yield and nitrous oxide outcomes for nitrogen management in agriculture.
1012 *Global Change Biology*, 27(11), 2343. <https://doi.org/10.1111/GCB.15588>
1013 Malcolm, B. J., Cameron, K. C., Curtin, D., Di, H. J., Beare, M. H., Johnstone, P. R., & Edwards, G. R.
1014 (2019). Organic matter amendments to soil can reduce nitrate leaching losses from livestock
1015 urine under simulated fodder beet grazing. *Agriculture, Ecosystems & Environment*, 272, 10–
1016 18. <https://doi.org/10.1016/J.AGEE.2018.11.003>
1017 Nguyen, T. H., Nong, D., & Paustian, K. (2019). Surrogate-based multi-objective optimization of
1018 management options for agricultural landscapes using artificial neural networks. *Ecological*
1019 *Modelling*, 400, 1–13. <https://doi.org/10.1016/j.ecolmodel.2019.02.018>
1020 Nielsen, O.-K., Plejdrup, M. S., Winther, M., Nielsen, M., Gyldenkærne, S., Mikkelsen, M. H.,
1021 Albrektsen, R., Thomsen, M., Hjelgaard, K. H., Fauser, P., Bruun, H. G., Johannsen, V. K., Nord-
1022 Larsen, T., Vesterdal, L., Callesen, I., Caspersen, O. H., Bentsen, N. S., Rasmussen, E.,
1023 Petersen, S. B., ... Hansen, M. G. (2020). *Denmark's National Inventory Report 2020: Emission*
1024 *Inventories 1990-2018 - Submitted under the United Nations Framework Convention on*
1025 *Climate Change and the Kyoto Protocol*.



- 1026 Pacheco, A. L., & Sumreen Hina, N. (2024). Global Meta-Analysis of Nitrate Leaching Vulnerability
1027 in Synthetic and Organic Fertilizers over the Past Four Decades. *Water* 2024, Vol. 16, Page
1028 457, 16(3), 457. <https://doi.org/10.3390/W16030457>
- 1029 Perlman, J., Hijmans, R. J., & Horwath, W. R. (2014). A metamodelling approach to estimate global
1030 N2O emissions from agricultural soils. *Global Ecology and Biogeography*, 23(8), 912–924.
1031 <https://doi.org/10.1111/geb.12166>
- 1032 Piñeros Garcet, J. D., Ordoñez, A., Roosen, J., & Vanclooster, M. (2006). Metamodelling: Theory,
1033 concepts and application to nitrate leaching modelling. *Ecological Modelling*, 193(3–4), 629–
1034 644. <https://doi.org/10.1016/j.ecolmodel.2005.08.045>
- 1035 Prokhorenkova, L., Gusev, G., Vorobev, A., Dorogush, A. V., & Gulin, A. (2017). *CatBoost: unbiased*
1036 *boosting with categorical features*. <https://doi.org/10.5555/3327757.3327770>
- 1037 Pugliese, L., Heckrath, G. J., Iversen, B. V., & Straface, S. (2023). Treatment Systems for Agricultural
1038 Drainage Water and Farmyard Runoff in Denmark: Case Studies. *Handbook of Environmental*
1039 *Chemistry*, 117, 45–65. <https://doi.org/10.1007/978-2021-784/FIGURES/7>
- 1040 Pylaniadis, C., Snow, V., Overweg, H., Osinga, S., Kean, J., & Athanasiadis, I. N. (2022). Simulation-
1041 assisted machine learning for operational digital twins. *Environmental Modelling and*
1042 *Software*, 148. <https://doi.org/10.1016/j.envsoft.2021.105274>
- 1043 Quemada, M., Baranski, M., Nobel-de Lange, M. N. J., Vallejo, A., & Cooper, J. M. (2013). Meta-
1044 analysis of strategies to control nitrate leaching in irrigated agricultural systems and their
1045 effects on crop yield. *Agriculture, Ecosystems & Environment*, 174, 1–10.
1046 <https://doi.org/10.1016/J.AGEE.2013.04.018>
- 1047 Rahimi, J., Haas, E., Scheer, C., Grados, D., Abalos, D., Aderere, M. O., Blicher-Mathiesen, G., &
1048 Butterbach-Bahl, K. (2024). Aggregation of activity data on crop management can induce
1049 large uncertainties in estimates of regional nitrogen budgets. *Npj Sustainable Agriculture*
1050 *2024 2:1*, 2(1), 1–10. <https://doi.org/10.1038/S44264-024-00015-3>
- 1051 Ren, K., Wang, Z., Wu, J., Zhao, K., Huang, M., & Li, Y. (2025). One-off irrigation enhances wheat
1052 yield and water productivity: Evidence from meta-analysis and a three-year and three-site
1053 field experiment. *Agricultural Water Management*, 317, 109628.
1054 <https://doi.org/10.1016/J.AGWAT.2025.109628>
- 1055 Rolighed, J. (2023). *Oparbejdning af landbrugsregisterdata og beregning af referenceudvaskning*
1056 *for nitrat med NLES5*. [https://pure.au.dk/portal/da/publications/oparbejdning-af-
1057 landbrugsregisterdata-og-beregning-af-referenceud/](https://pure.au.dk/portal/da/publications/oparbejdning-af-landbrugsregisterdata-og-beregning-af-referenceud/)
- 1058 Schuster, J., Mittermayer, M., Maidl, F. X., Nätscher, L., & Hülsbergen, K. J. (2022). Spatial
1059 variability of soil properties, nitrogen balance and nitrate leaching using digital methods on
1060 heterogeneous arable fields in southern Germany. *Precision Agriculture* 2022 24:2, 24(2),
1061 647–676. <https://doi.org/10.1007/S11119-022-09967-3>
- 1062 Shahhosseini, M., Martinez-Feria, R. A., Hu, G., & Archontoulis, S. V. (2019). Maize yield and nitrate
1063 loss prediction with machine learning algorithms. *Environmental Research Letters*, 14(12).
1064 <https://doi.org/10.1088/1748-9326/ab5268>
- 1065 Shcherbak, I., Millar, N., & Robertson, G. P. (2014). Global metaanalysis of the nonlinear response
1066 of soil nitrous oxide (N₂O) emissions to fertilizer nitrogen. *Proceedings of the National*
1067 *Academy of Sciences of the United States of America*, 111(25), 9199–9204.
1068 <https://doi.org/10.1073/PNAS.1322434111;PAGE=STRING:ARTICLE/CHAPTER>
- 1069 Shi, Y., Han, L., Zhang, X., Sobehi, T., Gaiser, T., Thuy, N. H., Behrend, D., Srivastava, A. K., Halder,
1070 K., & Ewert, F. (2025). *Deep Learning Meets Process-Based Models: A Hybrid Approach to*
1071 *Agricultural Challenges*. <https://arxiv.org/pdf/2504.16141>
- 1072 Shwartz-Ziv, R., & Armon, A. (2022). Tabular data: Deep learning is not all you need. *Information*
1073 *Fusion*, 81, 84–90. <https://doi.org/10.1016/J.INFFUS.2021.11.011>
- 1074 Slessarev, E. W., Mayer, A., Kelly, C., Georgiou, K., Pett-Ridge, J., & Nuccio, E. E. (2022). Initial soil
1075 organic carbon stocks govern changes in soil carbon: Reality or artifact? *Global Change*
1076 *Biology*, 29(5), 1239. <https://doi.org/10.1111/GCB.16491>



- 1077 Smerald, A., Kraus, D., Rahimi, J., Fuchs, K., Kiese, R., Butterbach-Bahl, K., & Scheer, C. (2023). A
1078 redistribution of nitrogen fertiliser across global croplands can help achieve food security
1079 within environmental boundaries. *Communications Earth and Environment*, 4(1).
1080 <https://doi.org/10.1038/s43247-023-00970-8>
- 1081 Styczen, M. E., Abrahamsen, P., Hansen, S., & Knudsen, L. (2020). Analysis of the significant drop
1082 in protein content in Danish grain crops from 1990-2015 based on N-response in fertilizer
1083 trials. *European Journal of Agronomy*, 115, 126013.
1084 <https://doi.org/10.1016/J.EJA.2020.126013>
- 1085 Sun, W., He, Z., Ma, D., Liu, B., Li, R., Wang, S., & Malekian, A. (2024). Response of soil carbon and
1086 nitrogen stocks to irrigation - A global meta-analysis. *Science of The Total Environment*, 957,
1087 177641. <https://doi.org/10.1016/J.SCITOTENV.2024.177641>
- 1088 Sutton, R. S., & Matheus, C. J. (1991). Learning Polynomial Functions by Feature Construction.
1089 *Proceedings of the 8th International Workshop on Machine Learning, ICML 1991*, 208–212.
1090 <https://doi.org/10.1016/B978-1-55860-200-7.50045-3>
- 1091 Vermeulen, S. J., Campbell, B. M., & Ingram, J. S. I. (2012). Climate change and food systems.
1092 *Annual Review of Environment and Resources*, 37(Volume 37, 2012), 195–222.
1093 <https://doi.org/10.1146/ANNUREV-ENVIRON-020411-130608/CITE/REFWORKS>
- 1094 Villa-Vialaneix, N., Follador, M., Ratto, M., & Leip, A. (2012). *Environmental Modelling and*
1095 *Software*. 34, 51–66. <https://doi.org/10.1016/j.envsoft.2011.05.003>
- 1096 Vogeler, I., Thomsen, I. K., Jensen, J. L., & Hansen, E. M. (2022). Marginal nitrate leaching around
1097 the recommended nitrogen fertilizer rate in winter cereals. *Soil Use and Management*, 38(1),
1098 503–514. <https://doi.org/10.1111/SUM.12673>
- 1099 Wang, C., Amon, B., Schulz, K., & Mehdi, B. (2021). Factors that influence nitrous oxide emissions
1100 from agricultural soils as well as their representation in simulation models: A review.
1101 *Agronomy*, 11(4), 770. <https://doi.org/10.3390/AGRONOMY11040770/S1>
- 1102 Wang, Y., Yao, Z., Zhan, Y., Zheng, X., Zhou, M., Yan, G., Wang, L., Werner, C., & Butterbach-Bahl,
1103 K. (2021). Potential benefits of liming to acid soils on climate change mitigation and food
1104 security. *Global Change Biology*, 27(12), 2807–2821. <https://doi.org/10.1111/GCB.15607>
- 1105 Weisberg, S. (2001). *Yeo-Johnson Power Transformations*. <http://www.stat.umn.edu/arc>.
- 1106 Wezel, A., Herren, B. G., Kerr, R. B., Barrios, E., Gonçalves, A. L. R., & Sinclair, F. (2020).
1107 Agroecological principles and elements and their implications for transitioning to sustainable
1108 food systems. A review. *Agronomy for Sustainable Development*, 40(6), 1–13.
1109 <https://doi.org/10.1007/S13593-020-00646-Z/FIGURES/5>
- 1110 Xiao, L., Wang, G., Wang, E., Liu, S., Chang, J., Zhang, P., Zhou, H., Wei, Y., Zhang, H., Zhu, Y., Shi,
1111 Z., & Luo, Z. (2024). Spatiotemporal co-optimization of agricultural management practices
1112 towards climate-smart crop production. *Nature Food*, 5(1), 59–71.
1113 <https://doi.org/10.1038/S43016-023-00891-X;SUBJMETA>
- 1114 Xiao, L., Wang, G., Zhou, H., Jin, X., & Luo, Z. (2022). Coupling agricultural system models with
1115 machine learning to facilitate regional predictions of management practices and crop
1116 production. *Environmental Research Letters*, 17(11). <https://doi.org/10.1088/1748-9326/ac9c71>
- 1117
- 1118 Yang, X., Xiong, J., Du, T., Ju, X., Gan, Y., Li, S., Xia, L., Shen, Y., Pacenka, S., Steenhuis, T. S., Siddique,
1119 K. H. M., Kang, S., & Butterbach-Bahl, K. (2024). Diversifying crop rotation increases food
1120 production, reduces net greenhouse gas emissions and improves soil health. *Nature*
1121 *Communications* 2024 15:1, 15(1), 198-. <https://doi.org/10.1038/s41467-023-44464-9>
- 1122 Yao, Z., Yan, G., Ma, L., Wang, Yan, Zhang, H., Zheng, X., Wang, R., Liu, C., Wang, Yanqiang, Zhu,
1123 B., Zhou, M., Rahimi, J., & Butterbach-Bahl, K. (2022). Soil C/N ratio is the dominant control
1124 of annual N₂O fluxes from organic soils of natural and semi-natural ecosystems. *Agricultural*
1125 *and Forest Meteorology*, 327, 109198. <https://doi.org/10.1016/J.AGRFORMET.2022.109198>



- 1126 Zhang, F., Qu, Z., Zhao, Q., Xi, Z., & Liu, Z. (2024). Mechanisms of N₂O Emission in Drip-Irrigated
1127 Saline Soils: Unraveling the Role of Soil Moisture Variation in Nitrification and Denitrification.
1128 *Agronomy 2025*, Vol. 15, Page 10, 15(1), 10. <https://doi.org/10.3390/AGRONOMY15010010>
1129 Zhang, N., Zhou, X., Kang, M., Hu, B. G., Heuvelink, E., & Marcelis, L. F. M. (2022). Machine learning
1130 versus crop growth models: an ally, not a rival. *AoB Plants*, 15(2), plac061.
1131 <https://doi.org/10.1093/AOBPLA/PLAC061>
1132 Zhou, L. T., Sun, S., Zhang, Z. T., Zhang, F. L., Guo, S. B., Shi, Y. Y., & Yang, X. G. (2022). High Yield
1133 and Water Use Efficiency Synergistical Improvement Irrigation Scheme of Winter Wheat in
1134 North China Plain Based on Meta-Analysis. *Chinese Journal of Agrometeorology*, 43(07), 515.
1135 <https://doi.org/10.3969/J.ISSN.1000-6362.2022.07.001>
1136 Žurovec, O., Wall, D. P., Brennan, F. P., Krol, D. J., Forrester, P. J., & Richards, K. G. (2021). Increasing
1137 soil pH reduces fertiliser derived N₂O emissions in intensively managed temperate
1138 grassland. *Agriculture, Ecosystems & Environment*, 311, 107319.
1139 <https://doi.org/10.1016/J.AGEE.2021.107319>
1140